

1

REVISED

2

3

**Dengue virus selectively annexes endoplasmic reticulum-associated translation**

4

**machinery as a strategy for co-opting host cell protein synthesis**

5

6 David W. Reid,<sup>a</sup> Rafael K. Campos,<sup>b,c</sup> Jessica R. Child,<sup>a</sup> Tianli Zheng,<sup>a</sup> Kittu Wing Ki  
7 Chan<sup>d,e</sup>, Shelton S. Bradrick,<sup>b</sup> Subhash G. Vasudevan<sup>d,e</sup>, Mariano A. Garcia-Blanco,<sup>b,d</sup>  
8 and Christopher V. Nicchitta<sup>a#</sup>

9

10 Department of Cell Biology, Duke University Medical Center, Durham, NC, USA<sup>a</sup>;  
11 Department of Biochemistry and Molecular Biology, University of Texas Medical Branch,  
12 Galveston, TX, USA<sup>b</sup>; Department of Molecular Genetics and Microbiology, Duke  
13 University Medical Center, Durham, NC, USA<sup>c</sup>; Programme in Emerging Infectious  
14 Diseases, Duke-NUS Medical School, Singapore<sup>d</sup>; Department of Microbiology, Yong  
15 Loo Lin School of Medicine, Singapore<sup>e</sup>

16

17 **Running title:** Dengue co-opts ER-associated translation

18

19 **#Address correspondence to:**

20 Christopher V. Nicchitta, PhD:

21 christopher.nicchitta@duke.edu

22

23 **Abstract:** 250 words

24 **Text:** 7,364 words

25 **Abstract**

26 A primary question in Dengue virus (DENV) biology is the molecular strategy for  
27 recruitment of host cell protein synthesis machinery. Here we combined cell  
28 fractionation, ribosome profiling, and RNA-seq to investigate the subcellular  
29 organization of viral genome translation and replication as well as host cell translation  
30 and its response to DENV infection. We report that throughout the viral life cycle, DENV  
31 (+) and (-) strand RNAs were highly partitioned to the endoplasmic reticulum (ER),  
32 identifying the ER as the primary site of DENV translation. DENV infection was  
33 accompanied by an ER compartment-specific remodeling of translation, where ER  
34 translational capacity was subverted from host transcripts to DENV (+) strand RNA,  
35 particularly at late stages of infection. Remarkably, translation levels and patterns in the  
36 cytosol compartment were only modestly affected throughout the experimental time  
37 course of infection. Comparisons of ribosome footprinting densities of the DENV (+)  
38 strand RNA and host mRNAs indicated that DENV (+) strand RNA was only sparsely  
39 loaded with ribosomes. Combined, these observations suggest a mechanism where  
40 ER-localized translation and translational control mechanisms, likely *cis*-encoded, are  
41 used to repurpose the ER for DENV virion production. Consistent with this view, we  
42 found ER-linked cellular stress response pathways commonly associated with viral  
43 infection, namely the interferon response and unfolded protein response, to be only  
44 modestly activated during DENV infection. These data support a model where DENV  
45 reprograms the ER protein synthesis and processing environment to promote viral  
46 survival and replication, while minimizing the activation of anti-viral and proteostatic  
47 stress response pathways.

48 **Importance**

49 DENV, a prominent human health threat with no broadly effective or specific treatment,  
50 depends on host cell translation machinery for viral replication, immune evasion, and  
51 virion biogenesis. The molecular mechanism by which DENV commandeers the host  
52 cell protein synthesis machinery and the subcellular organization of DENV replication  
53 and viral protein synthesis is poorly understood. Here we report that DENV has an  
54 almost exclusively ER-localized life cycle, with viral replication and translation largely  
55 restricted to the ER. Surprisingly, DENV infection largely affects only ER-associated  
56 translation, with relatively modest effects on host cell translation in the cytosol. DENV  
57 RNA translation is very inefficient, likely representing a strategy to minimize disruption  
58 of ER proteostasis. Overall these findings demonstrate that DENV has evolved an ER-  
59 compartmentalized life cycle and thus targeting the molecular signatures and regulation  
60 of the DENV-ER interaction landscape may reveal strategies for therapeutic  
61 intervention.

62 **Introduction**

63 The synthesis of viral proteins, which function in viral replication, evasion of immune  
64 defenses, and virion biogenesis, is wholly dependent on host cell translation machinery.  
65 Reflecting this need, viruses have evolved diverse strategies to out-compete cellular  
66 mRNAs and co-opt host translation capacity. Some viruses have evolved mRNAs that  
67 are translated by alternative mechanisms (e.g., IRES mediated, cap-independent  
68 translation initiation) and genes that modify or inactivate host cell factors required for  
69 cap-dependent host translation, thus providing mechanisms for viral RNAs to efficiently  
70 recruit ribosomes (1-6). Other viruses encode nucleases that specifically degrade host  
71 mRNAs, thereby significantly decreasing the competition of cellular translation activity  
72 (7). Yet others produce mRNAs that can, by nature of their extraordinary translation  
73 efficiency and/or high levels, outcompete most cellular mRNAs (8-10). As viral  
74 replication and viral protein synthesis is strictly dependent on the host cell translation  
75 machinery, understanding the mechanisms by which viruses promote translation of their  
76 RNAs within cells provides not only understanding of viral pathogenic mechanisms but  
77 also insights into host cell regulation of protein synthesis (11).

78 The mechanism by which Dengue virus (DENV), a member of the *Flavivirus* genus of  
79 RNA viruses and a prominent human pathogen, usurps host cell protein synthesis is  
80 largely unknown. Like all members of the genus *Flavivirus*, DENV contains an  
81 enveloped 5' m<sup>7</sup>GpppA-capped (+)-sense RNA genome with a nonpolyadenylated 3'  
82 untranslated region (UTR). The DENV 10.7 kb genome encodes a single polyprotein  
83 which is post-translationally cleaved into three structural (capsid [C], pre-  
84 membrane/membrane [prM/M], and envelope [E]) and seven nonstructural (NS1, NS2A,

85 NS2B, NS3, NS4A, NS4B, and NS5) proteins required for viral replication and  
86 inactivation of antiviral cellular pathways (12-14). Neither the structural nor nonstructural  
87 proteins are known to modify or compete with the cellular translation machinery. Indeed,  
88 earlier studies report little to no effect of DENV infection on total host cell protein  
89 synthesis (15, 16). Translation initiation of the DENV (+) strand RNA is thought to occur  
90 primarily through a canonical cap-dependent mechanism (17), although alternative  
91 strategies have been described when cap-dependent translation is inhibited (15).

92 DENV enters cells through receptor-mediated endocytosis (18) and gains access to the  
93 cytosol compartment following fusion of the viral envelope with the endosomal  
94 membrane. Having gained access to the cytosol, the viral genome then undergoes  
95 cycles of translation and replication that can produce upwards of 10,000 infectious  
96 particles per cell within 48 hours (19). Prior to the onset of viral replication, synthesis of  
97 the RNA-dependent RNA polymerase NS5, the RNA helicase NS3, and other NS  
98 proteins must occur, as these are required for assembly of the viral replication complex  
99 (20). Because (-) strand RNA synthesis and (+) strand translation compete for the same  
100 (+) strand template (21), the interplay between these two processes and their  
101 associated RNA structures is critical for optimal viral replication. Different long range  
102 RNA-RNA interactions appear to partition the genome between a linear form devoted to  
103 protein synthesis and a circular form focused on RNA transcription (22, 23), allowing for  
104 separation of these two processes in space and time.

105 DENV polyprotein and genome replication occurs in association with the endoplasmic  
106 reticulum (ER) (24). This intracellular membrane affiliation reflects both the nature of the  
107 polyprotein, which contains ca. twenty transmembrane domains and is dependent on

108 the ER protein translocation machinery for its biogenesis, and that many of the non-  
109 structural proteins, e.g. NS4A, behave as ER-resident membrane proteins and are  
110 principal components of ER-associated replication factories (24, 25). Correspondingly,  
111 DENV replication is highly sensitive to silencing or knock-out of host factors functioning  
112 in protein translocation and/or processing in the ER (26-28). Once the components of a  
113 viral particle have been synthesized, virions assemble and bud into the ER lumen,  
114 utilizing the secretory pathway to exit the cell (12).

115 Understanding how an ER-localized DENV (+) strand RNA serves as a template for  
116 temporally coordinated synthesis of both DENV (-) strand RNA and DENV proteins is  
117 important for understanding the DENV life cycle, yet our knowledge of these processes  
118 is limited. We considered this incomplete understanding in the context of our recent  
119 studies that point to distinct regulatory control of mRNA translation in the cytosol and  
120 ER (29-32) as well as transcriptome-wide functions for the ER-associated translation  
121 machinery in gene expression (30, 33). We thus paired ribosome profiling (34, 35) and  
122 RNA-Seq with biochemical cell fractionation (31, 36), to examine the subcellular  
123 organization of DENV translation through the viral life cycle. The overarching theme in  
124 the data is a DENV dependence on and selective modification of the ER-associated  
125 protein synthesis machinery. Three primary findings were revealed in this study. One,  
126 viral RNA, including the (-) strand replication template, and viral protein synthesis are  
127 wholly ER-compartmentalized. Second, DENV (+) strand RNA translation is highly  
128 inefficient relative to host cell mRNAs, suggesting a competition/selective capture  
129 mechanism for annexing host cell ER-associated ribosomes. Third, the host  
130 translational response to DENV infection is highly compartmentalized to the ER, as

131 most host ER-associated mRNAs are translationally suppressed, yet cytosolic host  
132 protein synthesis is relatively unchanged. Comparisons of transcriptome-wide changes  
133 in translation of host genes during DENV infection to the translational response evoked  
134 by the unfolded protein response (UPR) or treatment with interferon- $\beta$  (IFN)  
135 demonstrated that the host translation response to DENV included both UPR and IFN  
136 response pathways, and revealed a subset of genes whose translation is up-regulated  
137 during DENV infection. Interesting, we report that previously identified essential host  
138 factors for DENV infection are not translationally up-regulated during infection, but are  
139 rather generally repressed. These findings demonstrate that DENV specifically annexes  
140 ER-associated ribosomes, sacrificing synthesis of specific host proteins to maximize  
141 viral replication.

142 **Results**

143 **Tracking the subcellular compartmentalization of DENV genome replication and**  
144 **translation.**

145 The DENV 10.7 Kb (+) strand RNA, which encodes both cytosolic and integral  
146 membrane proteins, accesses the cytosol early in infection and is subsequently  
147 localized to the endoplasmic reticulum (ER), where it's translation products assemble  
148 replication and virion biogenesis centers (37, 38). As a first step towards understanding  
149 the molecular strategies used by DENV to commandeer host cell translation, we  
150 examined subcellular RNA distributions and the translational status of both host cell  
151 mRNAs and DENV (-) and (+) strand RNAs through the viral life cycle (36, 39). In  
152 combining the cell fractionation protocol illustrated in **Fig.1A**, which efficiently separates  
153 the two primary protein synthesis compartments of the cell, with RNA-seq and ribosome  
154 profiling, we sought to determine how DENV infection impacts the subcellular  
155 distribution and translation of host cell mRNAs, as it captures mRNA translation  
156 capacity and secretory pathway function, the latter for the production and secretion of  
157 new virions. In these experiments, Huh-7 hepatocarcinoma cells were infected with  
158 DENV (serotype 2; strain New Guinea-C) at a multiplicity of infection (MOI) of 10. After  
159 one hour, the viral inoculum was removed and the cells cultured for 6, 12, 24, or 40  
160 hours post infection (pi). At each time point, cells were fractionated using a sequential  
161 detergent-based fractionation method (**Fig. 1A**) (32, 36, 40). As illustrated, cells are first  
162 treated with a digitonin-supplemented physiological salts buffer, which selectively  
163 permeabilizes the plasma membrane and releases the cytosolic contents. The digitonin-  
164 extracted cells are then treated with n-dodecyl- $\beta$ -D-maltoside (DDM)-supplemented

165 buffers to release ER-associated cellular components. Similar to data reported in prior  
166 studies (39, 41-46), the immunoblot data in **Fig. 1B** demonstrate that the fractionation  
167 protocol yields the efficient separation and recovery of cytosolic (e.g., GAPDH, tubulin)  
168 and ER-resident (e.g., ribophorin I, TRAP $\alpha$ ) proteins, in both mock and DENV-infected  
169 cells. Note that DENV NS4B, an integral membrane protein, was wholly ER-associated  
170 in DENV-infected cells and absent from mock-infected cells (**Fig. 1B**). As expected,  
171 rRNAs (ribosomes) were recovered in both fractions, showing a modest ER-enrichment  
172 in mock-infected cells and an approximately equal subcellular distribution at 40 h post-  
173 infection (**Fig. 1C**). tRNAs, in contrast, were largely recovered in the cytosol fraction  
174 (**Fig. 1C**). The RNA component of the two subcellular fractions was analyzed by  
175 ribosome profiling (35), to assess mRNA translation status, and RNA-seq, to profile  
176 mRNA transcriptome composition (**Table S1**).

177 As depicted in **Fig. 2A**, the 40 hour time course captured the major phases of the DENV  
178 life cycle. DENV (+) strand RNA levels mirrored a logistic growth curve, with an  
179 apparent lag phase extending to approximately 12 hours followed by a replication  
180 phase. DENV (-) strand RNA levels, by contrast, steady increased until 24 hours post  
181 infection, followed by a decline. The relative levels of the DENV (+) strand, determined  
182 from the deep sequencing datasets, were approximately an order of magnitude higher  
183 than the DENV (-) strand throughout infection. We calculated the relative rates of (-) and  
184 (+) strand DENV RNA synthesis from the changes in RNA levels (**Fig. 2B**). Under the  
185 indicated experimental conditions, the peak rate of increase for the (+) strand RNA  
186 occurred between 12 and 24 h post-infection, with a doubling time of 20 min ( $\pm 3.8$  min).  
187 It should be noted that at an MOI of 10, each cell was likely exposed to  $\geq 1,000$  DENV

188 genomes, many of which could be defective in typical infections (47), thus likely  
189 lowering the calculated initial (+) strand synthesis rate. The pattern of change in (-)  
190 strand RNA levels differed markedly from (+) strand RNA, peaking early in infection and  
191 dropping throughout the remainder of the time course. The (-) strand RNA produced  
192 early in infected presumably serves as a subsequent template for robust (+) strand  
193 synthesis. These data identify an important temporal transition in the viral life cycle,  
194 where early periods of infection are weighted to (-) strand synthesis and later time  
195 periods to (+) strand synthesis and virion production.

196 We next investigated the subcellular localization of (-) and (+) strand RNA, as well as  
197 (+) strand translation, over the time course of infection (**Fig. 2C**). Both (-) and (+) strand  
198 RNAs were highly partitioned to the ER, where the (-) strand RNA remained almost  
199 entirely ER-bound throughout the time course despite not being translated. This finding  
200 may reflect localization of the (-) strand to ER-associated replication center and  
201 association with ER-associated template (+) strand. While the (+) strand is mostly ER-  
202 bound early in the infection, at late time points a discernible increase of (+) strand RNA  
203 in the cytosol was observed. The precise subcellular disposition of this fraction of (+)  
204 RNA is, however, not known, as at these late time points (+) strand RNA that scored as  
205 cytosolic includes maturing viral particles packaged within secretory pathway transport  
206 vesicles. In support of this interpretation, the translation of viral proteins remained highly  
207 ER-enriched at all time points, which is consistent with non-virion complexed (+) strand  
208 RNA being largely ER-associated throughout the experimental time course (**Fig. 2C**).

209 In addition to defining the subcellular locale of DENV translation, the ribosome profiling  
210 data allowed assessment of the translation status of the (+) RNA. Because DENV first

211 accesses the cytosol compartment in early infection, and subsequently uses the  
212 endoplasmic reticulum (ER) as a platform for virion production, we calculated the  
213 translation efficiency of the DENV (+) strand RNA in both the cytosolic and ER  
214 compartments, where translation efficiency is defined as the ribosome density within the  
215 coding sequence normalized to the level of the corresponding mRNA and is a proxy for  
216 mRNA translational status. The translation efficiency of cytosolic (+) strand RNA was  
217 low throughout the experimental time course. Intriguingly, for ER-bound DENV (+)  
218 strand RNA, translation efficiency is relatively low at the 6 h time point, but increases by  
219 12h post infection where it is sustained (data not shown). This period of relatively low  
220 translation efficiency on the ER overlaps with the period of high minus-strand synthesis  
221 rates, suggesting that at early infection, (+) strand translation is suppressed in favor of  
222 RNA replication. This transition may reflect a regulated transition from a primarily  
223 circularized, replication-dedicated (+) strand structure to a linearized, translationally-  
224 competent structure, as suggested previously (23, 48). Notably, even at the time points  
225 where DENV (+) strand RNA translation efficiency was highest, the relative translation  
226 efficiency was quite low relative to the host mRNA transcriptome, scoring in the bottom  
227 5<sup>th</sup> percentile (**Fig. 2D**). As we do not know the relative fraction of DENV (+) strand RNA  
228 engaged in transcription vs. translation, and whether the two processes are  
229 biochemically exclusive, the precise translation efficiency score cannot be stated with  
230 certainty. Nonetheless, these data suggest that the DENV (+) strand RNA is an  
231 intrinsically weak substrate for translation. The inefficiency of DENV translation may  
232 reflect, at least in part, its highly structured 5' UTR (49-51). There was essentially no  
233 detectable translation of the (-) strand RNA (**Fig. 2D**).

234 **Ribosome footprinting analysis of DENV (+) strand RNA translation reveals**

235 **intragenic variations in ribosome loading.**

236 To gain insight into the translational dynamics of the DENV (+) strand RNA, we  
237 examined the positional arrangement of the ribosome profiling reads over the ~ 10.3 Kb  
238 CDS at each time point in the experimental time course of infection (**Fig. 3A,C**). As  
239 depicted in **Fig. 3A**, ribosomes were broadly distributed along the CDS, with the  
240 prominent peaks and valleys that are typical of ribosome profiling data (35). The  
241 ribosome distribution pattern was largely unchanged over the experimental time course,  
242 suggesting that synthesis of a composite balance of structural and non-structural  
243 proteins is sustained throughout the infection cycle, which would be expected given the  
244 single ORF (**Fig. 3A-C**). In support of this conclusion, Pearson's correlation coefficients  
245 for ribosome densities between biological replicates were indistinguishable from  
246 comparisons between time points ( $r=0.85$  for replicates vs.  $0.87$  for comparisons;  $p$ -  
247 value= $0.35$  by two-tailed Student's t-test).

248 We next examined ribosome densities relative to the established N- and C-termini  
249 boundaries of the encoded proteins of the polyprotein, as a measure of intragenic  
250 translational variation (**Fig. 3C**). Such analyses are useful for defining alternative open  
251 reading frames, multiple ORFs, and ribosomal frame-shifting, as recently reported for  
252 the coronavirus, MHV, a (+) strand RNA virus (52). Programmed ribosomal frame  
253 shifting and/or multiple ORFs are not known to be strategies utilized by DENV (53, 54).  
254 Evident, however, are intragenic variations in ribosome density, where ribosome  
255 densities are lowest in the intragenic region encoding capsid and highest for the regions  
256 encoding NS2B, NS4B and NS5. Though relatively modest (net change  $< 1.5$  fold) the

257 intragenic variations in ribosome densities could arise through *cis*-encoded translational  
258 regulation, perhaps coupled to the ordered co-translational proteolytic processing of the  
259 DENV polyprotein into individual proteins (55, 56). The variations in ribosome density  
260 might also reflect a molecular strategy to compensate for differential stabilities of the  
261 processed proteins and so will require a detailed understanding of both intragenic  
262 ribosomal processivity and the stability/turnover rates of the individual processing-  
263 derived proteins to determine biological relevance.

264 A high number of RNA-seq reads mapped to the 3' UTR. These reads increased with  
265 time of infection and thus likely reflect production of the subgenomic flaviviral RNA  
266 (sfRNA) (57) (**Fig. 4**). This interpretation is supported by the lack of similar changes in 5'  
267 UTR RNA-seq map read densities as a function of time of infection. The sfRNA is a  
268 product of degradation of the viral genome by 5' to 3' exonucleases. The functions of  
269 the sfRNA in viral infection remain to be fully elucidated, but it is known to play a role in  
270 suppressing interferon stimulated genes expression, thus helping the virus evade the  
271 immune system. In contrast to the full DENV (+) strand RNA, the sfRNA was not highly  
272 enriched on the ER, consistent with previous work demonstrating functions for the  
273 sfRNA in the regulation of cytosolic anti-viral immunity factors (**Fig. 4B**) (58). Ribosome  
274 profiling reads mapping to the untranslated regions (UTR), particularly the 3' UTR were  
275 also obtained (**Fig. 3A**), but they were at a much lower density and their size distribution  
276 was discernibly different from other genes, suggesting that they likely represent  
277 nuclease protection by means other than ribosomes (e.g., RNA binding proteins, highly  
278 structured/nuclease resistant RNA domains), rather than translation (**Fig. 4C**).

279 **DENV infection predominantly remodels translation on the ER compartment.**

280 With the ribosome profiling data demonstrating that DENV (+) strand RNA translation  
281 was almost entirely localized to ER-bound ribosomes (**Fig. 2C**), we next examined the  
282 impact of viral RNA translation on global host cell protein synthesis, via the cell  
283 fractionation methodology introduced above. We first compared the relative abundance  
284 of ribosome footprint reads on ER-targeted mRNAs (mRNAs which encode an N-  
285 terminal hydrophobic signal sequence and/or transmembrane domains and are  
286 localized to the ER for translation and translocation) and cytosolic protein-encoding  
287 mRNAs (mRNAs which do not encode a signal sequence or transmembrane domain  
288 and are abundantly translated in the cytosol) (31, 33, 59, 60) (**Fig. 5A**). As illustrated in  
289 **Fig. 5A**, it was apparent that DENV infection resulted in time-dependent decrease in the  
290 translation of host ER-targeted mRNAs, beginning early in infection and progressing  
291 throughout the experimental infection period. In contrast, the translation of cytosol-  
292 encoding mRNAs was, on average, unchanged. As illustrated in **Fig. 5B**, analysis of the  
293 total RNA-seq datasets revealed that the levels of mRNAs encoding both ER-targeted  
294 and cytosolic proteins decreased somewhat over the course infection. The Ribo-Seq  
295 and RNA-seq analyses thus indicate that reductions in both ribosome loading and  
296 overall mRNA levels contribute to a reduction of total translation on the ER.

297 As previously reported, cytoplasmic protein-encoding mRNAs are broadly represented  
298 on the ER, though enriched in the cytosol compartment (31, 33, 59, 60). In the ER  
299 compartment specifically, the host ER-targeted mRNA cohort showed a 50% reduction  
300 in translation levels (**Fig. 5C**), whereas ER-associated cytosol-encoding mRNAs were  
301 only modestly altered (ca. 15% (**Fig. 5D**), indicating that the impact of DENV on ER-

302 associated translation was largely restricted to ER-associated secretory/membrane  
303 protein-encoding mRNAs. Because the DENV (+) strand RNA encodes ca. twenty  
304 transmembrane domains, its polyprotein translation product would be expected to  
305 compete with the translation products of host ER-targeted mRNAs for access to the  
306 protein translocation machinery. We thus further examined the impact of DENV infection  
307 on the translation of ER-targeted host mRNAs. To obtain a quantitative estimate of the  
308 impact of ER-localized DENV (+) strand RNA on the translation of ER-targeted host  
309 mRNAs, the RPKM values for ER-targeted mRNAs were multiplied by corresponding  
310 ORF length, to provide a measure of gene-specific ribosome abundance (**Fig. 5C**, see  
311 also **Fig. 5D**). This transformation accounts for the fact that ribosome loading is, in  
312 general, a function of ORF length; longer ORFs tend to be more populated with  
313 ribosomes and in this scenario occupy a greater fraction of the protein translocation  
314 machinery, then shorter ORFs (61, 62). Furthermore, with prior studies demonstrating  
315 that ribosomes engaged in the translation of secretory or transmembrane proteins are  
316 bound to the Sec61 protein translocation machinery, this metric provides a measure of  
317 the fractional utilization of the ER secretory capacity by this mRNA cohort (63-65). As  
318 depicted, by 24 h post-infection, DENV (+) strand RNA occupies similar levels of ER  
319 translocon-bound ribosomes as the host ER-targeted mRNAs and by 40 h post-  
320 infection, ribosome loading onto DENV (+) strand RNA surpassed ER-targeted host  
321 mRNAs, at which point the DENV (+) strand RNA had commandeered a majority of the  
322 ER secretory capacity (**Fig. 5C**). That the sum of the ER-targeted host mRNA and  
323 DENV (+) strand RNA ribosome abundance values at 40 h exceeds the ribosome  
324 abundance of ER-targeted host mRNAs at the zero time point is consistent with the

325 observation that DENV infection promotes expansion of the ER compartment, as  
326 previously reported, and thus an increase in total ER translocation activity and ribosome  
327 binding capacity (66).

328 To further explore the impact of DENV infection on host translation, [<sup>35</sup>S]Met/Cys pulse-  
329 labeling experiments were performed, again using the cell fractionation assay system  
330 depicted in **Fig. 1**. As a direct measure of *de novo* protein synthesis, [<sup>35</sup>S]Met/Cys  
331 pulse-labeling provides an orthogonal test of the ribosome footprinting data and  
332 distinguishes between translating and translationally-suppressed polyribosomes, which  
333 cannot be distinguished by ribosome footprinting alone. When combined with cell  
334 fractionation, this approach also reveals differences in the translational status of the  
335 cytosol and ER compartments (44, 46). In these experiments, Huh-7 cells were infected  
336 with DENV at an MOI of 10 and pulse-labeled with [<sup>35</sup>S] Met/Cys 36 h post-infection.  
337 Mock and DENV-infected cells were then fractionated and protein synthesis activity of  
338 the two compartments was assessed by phosphorimaging analysis of SDS-PAGE  
339 separated protein fractions (**Fig. 5E**). Total (unfractionated) cell extracts were obtained  
340 in parallel. As is evident in the total cell extracts, the impact of DENV infection on total  
341 proteome expression at the 36 h time point was substantial, with prominent DENV  
342 infection-dependent translation products present in the infected cells (**Fig. 5E**). The *de*  
343 *novo* translation patterns of the two subcellular fractions revealed distinct  
344 compartmental responses to DENV infection. Of particular interest, the overall  
345 translation pattern of the cytosol fraction at 36 h post-infection was very similar in the  
346 mock- and DENV-infected cells, with a modest suppression of overall translational  
347 activity (**Fig. 5E, Cyt Frac**) (67). Clearly evident in the cytosol fraction of the infected

348 cells was a radiolabeled band of ca. 100 kDa, which is the predicted mobility of NS5, the  
349 methyltransferase-polymerase (68). Lacking transmembrane domains and/or a signal  
350 peptide, NS5 would be expected to be highly enriched in the cytosol fraction, however a  
351 fraction was recovered in the ER fraction as well, which may represent NS5 polymerase  
352 associated with ER-bound (-) strand DENV RNA. The identity of the DENV infection-  
353 specific radiolabeled band migrating slightly faster than the 100 kDa remains to be  
354 determined. Contrasting with the cytosol fraction, DENV-infection elicited a dramatic  
355 remodeling of the ER-associated proteome. Previously abundant ER proteins were  
356 scarcely detectable and DENV proteins instead dominated the output of ER protein  
357 biosynthesis (**Fig. 5E, ER Frac**). Of particular interest is the radiolabeled protein of ca.  
358 68 kDa, present in the ER fraction and absent from the cytosol fraction of DENV-  
359 infected cells. The mobility of this protein in SDS-PAGE is consistent with the  
360 processing protease NS3. As NS3 lacks a signal sequence or transmembrane domain  
361 (69), it would be predicted to reside in the cytosol. Prior studies have established that  
362 NS3 associates with NS2B to form the active processing protease; with NS2B being an  
363 integral membrane protein localized to the ER, this protein-protein interaction would be  
364 expected to confer ER localization to soluble NS3 (68, 70, 71). To further explore these  
365 findings, immunoblot analyses of DENV capsid, envelope, prM, NS2B, NS3, and NS5  
366 expression and subcellular localization were performed (**Fig. 5F**). As shown, the  
367 immunoblot studies were consistent with the data depicted in Fig. 5E and directly  
368 demonstrate both viral protein expression and subcellular localization.

369 Combined with the ribosome footprinting data, the [<sup>35</sup>S]Met/Cys pulse-labeling and  
370 DENV protein immunoblot data illustrate that DENV primarily commandeers ER

371 translocon-associated ribosomes and suppresses translation of ER-targeted host  
372 mRNAs. Furthermore, analyses of the relative distribution of ER-bound ribosomes  
373 engaged in the translation of DENV (+) strand RNA and ER-targeted mRNAs reveal a  
374 slow process of ribosome capture by the DENV (+) strand RNA, occurring  
375 approximately in parallel with the synthesis of (+) strand DENV RNA (**Figs. 2A, 5C**).

### 376 **Global translation response to DENV infection**

377 The changes in mRNA translation patterns reported above were apparent at a  
378 transcriptomic scale. Heat map analysis of the ribosome footprinting data sets indicated  
379 a broad spectrum of altered translation by 40 h infection, though translation was largely  
380 unaffected at earlier time points when DENV (+) strand RNA levels are relatively low  
381 (**Fig. 6A**). Using a cutoff of two-fold change in total translation at the 40 h point, 948  
382 mRNAs had enhanced translation and 880 mRNAs had suppressed translation.  
383 Importantly, the changes in translation status seen at early infection time points largely  
384 reflected lower-magnitude variants of the late infection time points. While there are  
385 specific genes that are expressed early in response to DENV infection, the majority of  
386 changes in host mRNA translation in response to DENV represent a conserved,  
387 progressive response that increases in magnitude over the time course of infection (**Fig.**  
388 **6A**).

389 To assess the mechanisms driving these changes in gene expression, we first queried  
390 the roles of two gene expression programs known to be active during DENV infection:  
391 the interferon (IFN) pathway and the Unfolded Protein Response (UPR) (72). We  
392 defined a set of IFN-stimulated genes by treatment of Huh-7 cells with IFN- $\beta$  for 12  
393 hours. An orthologous UPR-responsive gene set was derived from a previous ribosome

394 profiling study that used thapsigargin treatment of mouse embryonic fibroblasts to elicit  
395 UPR activation (42). In comparing the changes in these gene sets over the course of  
396 DENV infection, each was significantly increased, indicating that the two pathways  
397 were, as expected, up-regulated (**Fig. 6B**). With regard to UPR-responsive genes,  
398 induction was quite slow and modest, more consistent with a supportive role for the  
399 UPR, e.g., expansion of ER secretory capacity, rather than an acute, proteostatic stress  
400 response (67, 73, 74). A Venn diagram of these data sets revealed a significant overlap  
401 ( $p < 0.005$  for all; hypergeometric test) between genes with enhanced expression in  
402 DENV infection and both IFN induced and UPR pathways (**Fig. 6C**). However, there  
403 remained a substantial cohort of mRNAs (433) whose translation was enhanced during  
404 DENV infection, but not by IFN or UPR, which we term the DENV-only gene set (**Table**  
405 **S2**). These genes may represent specific host cell responses to infection or changes in  
406 gene expression driven by DENV itself. Gene ontology analysis of the 433 DENV-only  
407 genes revealed the most significant biological processes link to the GO categories  
408 autophagy, regulation of cell cycle, signal transduction, and cellular metabolism (**Fig.**  
409 **6D, Table S3**).

410 DENV-only and IFN-induced genes differed from the rest of the transcriptome in their  
411 means of activation (**Fig. 6E**). While most transcriptome-wide changes in total  
412 translation were driven by changes in mRNA levels, changes in DENV-only genes and  
413 IFN-induced genes were primarily driven by changes in translational efficiency. The  
414 activation of the UPR was primarily transcriptional, likely through the activation of the  
415 UPR-linked transcription factors XBP-1, ATF4 and CHOP (75-77).

416 Given the ER-centric translational response to DENV described thus far and recent  
417 CRISPR screens for flaviviral host factors identifying primarily ER-resident proteins (27,  
418 28), we examined how DENV infection affects the expression of high confidence DENV  
419 host factors. We focused our analysis on the Marceau, et al. (27) screen as it utilized  
420 DENV serotype 2 and Huh-7 cells, as in the current study (**Table S4**) (27). This analysis  
421 revealed many of the CRISPR-identified essential host factors to be translationally  
422 down-regulated, whereas host genes were on average unchanged (**Fig. 7A**).  
423 Specifically, of the 23 ER-resident CRISPR-identified host factor genes also present in  
424 our ribosome footprinting data set, 17 genes were translationally down-regulated at 40 h  
425 post infection ( $\log_2[40h/uninfected] < 0$ ) and 6 were translationally up-regulated  
426 ( $\log_2[40h/uninfected] > 0$ ), though this host factor gene set is not substantially or up- or  
427 down-regulated (**Fig. 7B**). Non-ER-resident CRISPR-identified host factors did not have  
428 a particular bias for up or down regulation (5 genes and 4 genes, respectively). The  
429 same trends in changes to translation for these CRISPR-identified host factors were  
430 seen at earlier time points, though to a lesser magnitude, as was observed with global  
431 translational changes (**Fig. 6A**). It is also of note that the changes in translation of  
432 CRISPR-identified host factors during DENV infection do not correlate with changes in  
433 their RNA levels, suggesting transcript-specific regulation of translation (**Table S1**).

434 **Discussion**

435 Whereas the general trajectory and biochemical machinery of DENV replication are  
436 increasingly well-understood (12, 78), major gaps in our understanding of how DENV  
437 coordinately regulates the synthesis of its RNAs and proteins remain. In addition, the  
438 fundamental question of how DENV (+) strand RNA competes for host cell translation  
439 capacity is largely unknown. Here, we mapped the landscape of transcriptional and  
440 translational responses to DENV infection in the host, and mapped the succession and  
441 subcellular organization of the RNA replication and protein synthesis events that define  
442 the DENV life cycle. DENV executes a major annexation of translation on the ER,  
443 substantially reducing the translation of most host ER-targeted mRNAs. In addition to  
444 sequestering ER-associated ribosomes, the very low translation efficiency of DENV (+)  
445 strand RNA identified here may represent a strategy for minimizing the proteostatic  
446 stress on the ER protein folding machinery, thereby limiting activation of the unfolded  
447 protein response, with its attendant PERK-mediated suppression of cap-dependent  
448 translation and general protein synthesis (79).

449 Combining the findings obtained in RNA-seq and Ribo-seq analysis of RNA abundance  
450 and translational status in the cytosol and ER compartments of DENV-infected human  
451 cells, a temporal order of molecular events was documented. Following viral RNA entry  
452 into the cytosol, the primary activity of DENV is (-) strand RNA synthesis. This activity,  
453 however, must be preceded by (+) strand translation for synthesis of the NS5 RNA  
454 polymerase. Once a critical concentration of DENV proteins is accumulated, the early  
455 commitment to (-) strand RNA synthesis serves as an investment that supports (+)  
456 strand replication and virion biogenesis. As infection progresses, (-) strand RNA

457 synthesis drops and is replaced by two primary functions: robust translation of (+) strand  
458 RNA and rapid synthesis of additional (+) strand RNA from the now-abundant (-) strand  
459 template. Following the continued buildup of DENV proteins and RNA, a population of  
460 untranslated (ribosome-free) (+) strand RNA begins to populate the cytosol, likely  
461 representing virions in the process of secretion. These data therefore reinforce the  
462 concept that the two functions of the (+) DENV RNA – a template for (-) strand synthesis  
463 and a mRNA for translation – are in direct competition, and are temporally skewed;  
464 synthesis of (-) strand RNA from the (+) strand template is prioritized through the 6 h  
465 time point, whereas translation of the (+) strand dominates thereafter.

466 The critical processes of DENV protein and RNA synthesis are contingent upon the  
467 virus's ability to co-opt the structure and activity of the ER. Data included here  
468 demonstrate the localization of the vast majority of the viral RNA to the ER, including  
469 the (-) strand RNA, which is untranslated and not captured in nascent viral particles.  
470 Strikingly, and as further evidence of the importance of an ER-restricted life cycle,  
471 DENV RNAs were enriched on the ER to a degree greater than host ER-targeted  
472 mRNAs (43), suggesting that there exist DENV-specific mechanisms for ensuring the  
473 highly efficient partitioning and anchoring of the (+) strand RNA to the ER. Non-  
474 structural DENV proteins, many of which are themselves integral membrane proteins,  
475 may serve important functions in this RNA anchoring process. It is also possible that  
476 DENV co-opts previously identified host cell factors that function in mRNA anchoring to  
477 the ER (40, 80, 81).

478 Given the intricate nature of DENV transmembrane domain synthesis and the complex  
479 polytopic topology of the polyprotein, the low translational efficiency of DENV RNA

480 identified here may be adaptive, as it could serve as a “kinetic trap” and thereby divert  
481 ribosomes from host mRNAs to the DENV (+) strand RNA translation. Such inefficient  
482 translation may also be adaptive from the viewpoint of ER proteostasis. Were, for  
483 example, (+) strand RNA translation to be highly efficient, the increased protein folding  
484 load on the ER would be expected to trigger activation of the UPR, leading to  
485 suppression of protein synthesis. In contrast, inefficient translation as an adaptive  
486 feature would allow for abundant (+) strand RNA for virion production while avoiding  
487 deleterious levels of UPR activation. Here we do not observe an acute or pronounced  
488 activation of the UPR, but rather a slow increase in the transcription and translation of  
489 select UPR-associated genes (**Fig. 6B and 6C**). Such a model would be consistent with  
490 earlier findings that DENV infection intersects with the UPR pathway in complex and  
491 temporally selective manner (67). The inefficiency of DENV translation likely reflects, at  
492 least in part, its highly structured 5' UTR and a low rate of translation initiation (50, 82).  
493 These characteristics distinguish DENV (+) strand RNA from other (+) strand RNA  
494 viruses, such as the corona virus MHV, whose single stranded RNA genome is  
495 translated at an efficiency similar to host transcripts (83).

496 The means by which DENV controls host gene expression also reveals a highly ER-  
497 centric strategy. Over the course of DENV infection, non-DENV membrane protein  
498 synthesis is reduced at multiple levels. Thus, on the ER there is a significant reduction  
499 in the translation of these host mRNAs relative to mRNAs encoding cytosolic proteins  
500 that are also translated on ER-bound ribosomes (30, 39, 43, 84). Although there is a  
501 modest impact on host translation generally, the impact that DENV has specifically on  
502 host ER translation is large and broadly inhibitory, including a set of previously identified

503 essential host factors (discussed below). While these findings bear similarity to those  
504 recently reported by Roth and coworkers (85), the two studies differ in conclusions  
505 regarding the overall magnitude of the translational inhibition observed in response to  
506 DENV infection. These differences likely reflect different assay systems used to assess  
507 translation and in that regard we note that the magnitude of translational suppression  
508 reported by Roth and coworkers via ribopuromycylation assay is similar to that reported  
509 here by [<sup>35</sup>S] Met/Cys incorporation and compartmental analysis of translation via Ribo-  
510 seq.

511 The exceptions to the trend of suppressed translation hints at an important role for  
512 translational regulation of host mRNAs by DENV itself, e.g., the enhanced translation of  
513 mRNAs encoding components of the secretory pathway likely increases the cellular  
514 capacity for secreting DENV virions. How this is accomplished awaits further study and  
515 speaks to the emerging view of the ER as a central hub participating in the translation of  
516 the mRNA transcriptome, with mRNAs localized and anchored by diverse mechanisms,  
517 and the capacity for selective regulation of the translation of mRNA subsets (30).

518 The view that DENV-directed translational changes contribute to the remodeling of host  
519 cell gene expression is supported by comparison of the ribosome footprinting data of  
520 cells infected with DENV versus cells treated with IFN- $\beta$  or thapsigargin, which activate  
521 interferon response pathways or UPR, respectively. These two cellular response  
522 pathways are associated with flavivirus infection and could be the driving factors for the  
523 translational responses observed during DENV infection (Fig. 6). In this comparison of  
524 transcriptionally activated genes, however, only subsets of IFN-activated and UPR-  
525 associated genes are translationally up-regulated during DENV infection. The “DENV

526 only” subset of genes is generally related to regulation of catabolic processes (**Table**  
527 **S3**). These biological processes could ultimately favor viral replication and virion  
528 production by dedicating cellular anabolic activities toward the viral life cycle, replication  
529 of viral RNA, and folding and packaging of viral proteins. It should be considered that  
530 the specific genes found in the “DENV only” category (Table S2) may be used most  
531 directly by the virus during its lifecycle and could comprise therapeutic targets.

532 The high confidence links between ER physiology and the DENV viral lifecycle  
533 discussed above was also observed in recent genome-wide CRISPR screens for  
534 essential flavivirus host factors (27, 28). Interestingly, many of the identified DENV2  
535 host factors in these past studies were found to be translationally repressed in our data  
536 sets. Though somewhat counterintuitive, this pattern may suggest a novel way of  
537 evaluating how pathogens utilize host factors. In a genetic deletion screen, as  
538 referenced here, cells experience a complete loss of gene function before they  
539 encounter a pathogen. During infection of non-genetically modified cells, however, cells  
540 are fully equipped with essential host factors at the start of infection. After the initial  
541 infection, two response branches are likely to occur: 1) cells may respond by down-  
542 regulating specific factors as a strategy to combat the infection or 2) the virus may  
543 evoke strategies to up-regulate host factors that are beneficial to its survival. As the  
544 virus has already gained access to the cell, and replication and translation have begun  
545 before the cell is able to detect and respond to the infection, the evolutionary pressure  
546 to develop a mechanism that prevents host translational repression is likely low for most  
547 genes. In this way, the virus likely allows for the translational down regulation of host  
548 factors required early in infection. It is also likely the virus has developed strategies to

549 upregulate specific factors that are required throughout the viral life cycle. By this logic,  
550 host factors identified by loss-of-function that are translationally repressed during  
551 infection may be therapeutically relevant targets to minimize or block initial infection,  
552 whereas host factors that are translationally activated during infection may impact viral  
553 success at later stages of infection (i.e. when an individual is already infected). This  
554 proposed bimodal evaluation of host factors, which considers not only the outcome of  
555 the virus but how the protein is regulated during infection, will require experimental  
556 validation but may provide an opportunity for insight into the questions of how and when  
557 a host factor contributes to the viral life cycle.

558 Cumulatively, these findings highlight the ER as not only the site of viral replication, but  
559 as an organelle that DENV dramatically remodels to fulfill the need for both biogenesis  
560 and an exit strategy from the cell. This viral habitat provides not only entry into the  
561 secretory pathway, but also a distinct environment for translational regulation that DENV  
562 controls to optimize conditions for replication (30, 86, 87). Targeting any of these points  
563 where DENV interacts with or controls the ER may be a promising area to explore anti-  
564 viral pharmaceuticals.

565 **Materials and Methods**

566 **Cells and viruses**

567 Huh-7 (human hepatocarcinoma cells, ATCC) were grown in 4.5g/L glucose DMEM  
568 (Gibco, USA), supplemented with 10% FBS, non-essential amino acids (Gibco, USA),  
569 100 U/ml penicillin and 100 µg/ml streptomycin (Gibco, USA). Cells were cultured at  
570 37°C in a humidified 5% CO<sub>2</sub> incubator. DENV strain DENV2-NGC (GenBank accession  
571 M29095.1) was used for experiments. Viruses were grown in C6/36 cells and titered by  
572 standard Vero foci forming assay.

573 **Viral infection protocol**

574 Huh-7 cells were plated at a density of 2x10<sup>6</sup> cells per 10cm<sup>2</sup> dish. Cells were infected  
575 with DENV-2 NGC strain at a MOI (multiplicity of infection) of 10 for 1h, the virus  
576 inoculums were then removed and cells washed once with PBS before replacing with  
577 pre-warmed complete media. MOIs were calculated using Vero cell-based titers as  
578 noted above. Interferon treatment was performed using recombinant Interferon beta 1A  
579 (Millipore) for 12 hours at 500 units/mL.

580 **Cell fractionation**

581 Cells were treated with 180µM cycloheximide for 30 seconds then washed with cold  
582 PBS. Cells were then separated into their cytosolic and ER compartments as previously  
583 described (39, 43, 45, 84, 88, 89). Briefly, the cytosol fraction was extracted by addition  
584 of a buffer containing 0.03% digitonin, 110 mM KOAc, 25 mM K-HEPES pH 7.2, 15 mM  
585 MgCl<sub>2</sub>, and 4 mM CaCl<sub>2</sub> to the dish and incubated in ice for 5 min. The buffer was  
586 collected, and cells washed with the same buffer containing 0.0015% digitonin. The first  
587 lysis and the wash were combined and represent the cytosolic contents of the cell. The

588 ER fraction was then collected by lysis of the digitonin-extracted cells with an ER lysis  
589 buffer containing 2% n-dodecyl- $\beta$ -D-maltoside, 200 mM KOAc, 25 mM K-HEPES pH  
590 7.2, 15 mM MgCl<sub>2</sub>, and 4 mM CaCl<sub>2</sub>.

#### 591 **Ribosome profiling and RNA-seq**

592 Cell lysates were diluted to 100 mM KOAc and treated with 10  $\mu$ g/mL micrococcal  
593 nuclease for 30 min at 37°C. Ribosomes were pelleted by ultracentrifugation through a  
594 0.5M sucrose cushion in a Beckman TL100 ultracentrifuge, using the TLA100.2 rotor  
595 (24 min, 90,000 RPM). Ribosomal pellets were subjected to phenol/chloroform  
596 extraction, the RNA isolated, and subsequently treated with polynucleotide kinase (New  
597 England Biolabs). Ribosome-protected mRNA fragments were then size-selected by  
598 acrylamide gel electrophoresis, extracted, and assembled into cDNA libraries as  
599 described in previous publications from this lab and summarized below (42, 90).

600

601 For mRNA-seq, total RNA was isolated from lysates by phenol/chloroform extraction.  
602 rRNA was depleted using RiboZero (Illumina). Eluted mRNA was fragmented by  
603 resuspending in 100  $\mu$ L 40 mM Tris-OAc pH 8.3, 100 mM KOAc 30 mM MgOAc and  
604 heating to 95°C for 10 min. Fragmented RNA was precipitated by addition of NaOAc to  
605 300 mM and 300  $\mu$ L ethanol, the solution chilled on ice, and RNA collected by  
606 centrifugation. The RNA pellet was resuspended in a 10  $\mu$ L solution containing 10 mM  
607 ATP, 10 U polynucleotide kinase (New England Biolabs), and 1 X PNK buffer. This  
608 solution was incubated at 37 °C for 30 minutes, then heat inactivated at 95 °C for 10  
609 min.

610 Each of the RNA fragment pools was converted into a cDNA library using the NEBNext  
611 Small RNA Library Prep Set for Illumina (New England Biolabs) as described by the  
612 manufacturer, except using half reactions. cDNA libraries were amplified using 16  
613 cycles of PCR, then pooled and sequenced using the HiSeq 2500 (Illumina). Reads are  
614 available under Gene Expression Omnibus Accession GSE69602.

615 **Analysis of protein and RNA compositions of subcellular fractions.**

616 Huh-7 cells were mock-infected or DENV-infected (MOI = 10) and fractionated into  
617 cytosol and endoplasmic reticulum (ER) fractions as described above. Fractions were  
618 either subjected to trichloroacetic acid precipitation, to recover the protein fraction, or  
619 extracted with Trizol® to obtain the total RNA fraction. To analyze protein distributions in  
620 the two subfractions, samples were resuspended in SDS-PAGE sample buffer,  
621 separated on 12.5% SDS-PAGE gels, transferred to nitrocellulose membranes and  
622 protein distributions analyzed by immunoblot using the following monoclonal antibodies  
623 GAPDH: DSHB-hGAPDH-2G7; tubulin: 6G7; and rabbit polyclonal antisera recognizing  
624 ribophorin I and TRAP $\alpha$ . Monoclonal antibodies were obtained from the Developmental  
625 Studies Hybridoma Bank, created by the NICHD of the NIH and maintained at The  
626 University of Iowa, Department of Biology, Iowa City, IA 52242. Rabbit antisera were  
627 generated by immunization with KLH-synthetic peptide conjugates and were  
628 characterized in prior reports from the Nicchitta laboratory (39, 41, 88). For analysis of  
629 viral protein expression, Huh7 cells were plated at  $3 \times 10^5$  cells in a six-well dish and  
630 infected the following day with DENV-2 (NGC) MOI of 10, as described above. Infection  
631 was allowed to carry on for 36 h and then cells were fractionated into cytoplasmic and  
632 ER fractions as described above. Proteins were TCA precipitated and re-suspended in

633 1x LDS loading buffer (Novex). Proteins were heated at 95°C for 5 minutes, and the  
634 same volume of lysate for each compartment was separated on a 4-12% SDS-PAGE  
635 gel (Novex), the proteins transferred to nitrocellulose membranes, and expressed  
636 proteins detected using antibodies against C, prM, E, NS1, NS2B, NS4B, NS3 or NS5  
637 (Genetex) and fluorescence-based detection (LI-COR).

638 To assess RNA compositions, samples were separated on agarose gels, stained with  
639 SYBR® Green II, and imaged on a GE Healthcare Amersham Imager 600.

#### 640 **Metabolic labeling of tissue culture cells**

641 Huh-7 cells were plated at  $3 \times 10^6$  cells per well in a six-well dish and infected as above.  
642 At the end of infections, cells were incubated in methionine and cysteine free media for  
643 30 minutes to deplete internal pools of these amino acids. Cells were then labeled by  
644 addition of 0.2 mCi/mL [ $^{35}\text{S}$ ]Met/Cys media for 30 minutes, washed with PBS three  
645 times, and lysed with a buffer consisting of 400 mM KOAc, 15mM Mg(OAc)<sub>2</sub>, 25 mM  
646 HEPES, pH 7.6, 1% NP-40, and 1 mM DTT. Proteins were TCA precipitated and  
647 resuspended in 1x LDS loading buffer (Novex). Proteins were separated on a 4-12%  
648 acrylamide gel (Novex), dried, and the gels were phosphorimaged using a GE Typhoon  
649 Trio.

#### 650 **Data analysis**

651 Reads were first trimmed of their 3' adapters using Cutadapt (91). A reference  
652 transcriptome was generated with Tophat and Cufflinks (92), using combined RNA-seq  
653 data to generate a consensus transcriptome from Refseq release 68. The most  
654 abundant isoform of each gene was selected and compiled into a reference

655 transcriptome. All reads were then mapped using Bowtie (93), allowing no mismatches.  
656 Reads within the coding sequence were counted and normalized by coding sequence  
657 length and library size to give total translation and mRNA counts. Genes where fewer  
658 than 4 reads were mapped were discarded for that sample. sfRNA levels were  
659 determined via the equation (3' UTR read density/CDS read density) x RPKM (DENV  
660 CDS).

661 To calculate the rates of change in DENV RNA levels, changes in RNA levels were  
662 fitted to an exponential growth model  $y_{t+1} = y_t \times e^{k\Delta t}$ , where  $y$  is the RNA level time  $t$  and  
663  $k$  is the growth rate. This equation was solved for  $k$  and converted to a percentage:

$$664 \quad k = 100 \times \ln\left(\frac{y_{t+1}}{y_t}\right) / \Delta t .$$

665 Relative contributions of mRNA levels and ribosome loading to overall changes in  
666 ribosome footprinting data were performed as described in (94), where the percentage  
667 of change driven by mRNA levels is calculated by the geometric mean of correlations  
668 between RNA-seq fold changes and ribosome footprinting fold changes, divided by the  
669 correlations between ribosome footprinting replicates. Changes in ribosome loading are inferred  
670 to contribute the remainder of the fold change.

671 All sequencing data are available at GEO accession number GSE69602.

672

673

674 **Acknowledgements**

675 We thank the members of the Nicchitta, Garcia-Blanco, and Vasudevan labs, as well as  
676 Shirish Shenolikar at Duke-NUS Medical School, for providing an energizing intellectual  
677 environment and critical feedback on the manuscript. This work was supported through  
678 Duke/Duke-NUS Research Collaboration Awards 2014/0013 and 2016/0025 (CVN and  
679 SGV), NMRC/MOHIAFCat1/0018/2014 (SGV), NIH RO1AI089526 and RO1AI101431  
680 (MAGB), and NIH GM101533-05A1 and NIH GM118630-01A1 (CVN). We thank Shirish  
681 Shenolikar, Duke-NUS, for partial funding of salary support for DR and the National  
682 Science Foundation Graduate Research Fellowship Program Grant No. DGS-1644868  
683 for funding tuition and stipend for JC. The funders had no role in study design, data  
684 collection and analysis, decision to publish, or preparation of the manuscript. Any  
685 opinions, findings, and conclusions or recommendations expressed in this material are  
686 those of the author(s) and do not necessarily reflect the views of the National Science  
687 Foundation.

688 **References**

- 689 1. **Gingras AC, Svitkin Y, Belsham GJ, Pause A, Sonenberg N.** 1996. Activation  
690 of the translational suppressor 4E-BP1 following infection with  
691 encephalomyocarditis virus and poliovirus. *Proceedings of the National Academy  
692 of Sciences of the United States of America* **93**:5578-5583.
- 693 2. **Borman AM, Michel YM, Kean KM.** 2001. Detailed analysis of the requirements  
694 of hepatitis A virus internal ribosome entry segment for the eukaryotic initiation  
695 factor complex eIF4F. *Journal of virology* **75**:7864-7871.
- 696 3. **Kuyumcu-Martinez M, Belliot G, Sosnovtsev SV, Chang KO, Green KY,  
697 Lloyd RE.** 2004. Calicivirus 3C-like proteinase inhibits cellular translation by  
698 cleavage of poly(A)-binding protein. *Journal of virology* **78**:8172-8182.
- 699 4. **Komarova AV, Real E, Borman AM, Brocard M, England P, Tordo N,  
700 Hershey JW, Kean KM, Jacob Y.** 2007. Rabies virus matrix protein interplay  
701 with eIF3, new insights into rabies virus pathogenesis. *Nucleic acids research*  
702 **35**:1522-1532.
- 703 5. **He B, Gross M, Roizman B.** 1997. The gamma(1)34.5 protein of herpes simplex  
704 virus 1 complexes with protein phosphatase 1alpha to dephosphorylate the alpha  
705 subunit of the eukaryotic translation initiation factor 2 and preclude the shutoff of  
706 protein synthesis by double-stranded RNA-activated protein kinase. *Proceedings  
707 of the National Academy of Sciences of the United States of America* **94**:843-  
708 848.
- 709 6. **Aoyagi M, Gaspar M, Shenk TE.** 2010. Human cytomegalovirus UL69 protein  
710 facilitates translation by associating with the mRNA cap-binding complex and  
711 excluding 4EBP1. *Proceedings of the National Academy of Sciences of the  
712 United States of America* **107**:2640-2645.
- 713 7. **Abernathy E, Gilbertson S, Alla R, Glaunsinger B.** 2015. Viral Nucleases  
714 Induce an mRNA Degradation-Transcription Feedback Loop in Mammalian Cells.  
715 *Cell host & microbe* **18**:243-253.
- 716 8. **Walsh D, Mathews MB, Mohr I.** 2013. Tinkering with translation: protein  
717 synthesis in virus-infected cells. *Cold Spring Harbor perspectives in biology*  
718 **5**:a012351.
- 719 9. **Leong K, Lee W, Berk AJ.** 1990. High-level transcription from the adenovirus  
720 major late promoter requires downstream binding sites for late-phase-specific  
721 factors. *Journal of virology* **64**:51-60.
- 722 10. **Guarino LA, Summers MD.** 1986. Interspersed Homologous DNA of  
723 *Autographa californica* Nuclear Polyhedrosis Virus Enhances Delayed-Early  
724 Gene Expression. *Journal of virology* **60**:215-223.
- 725 11. **Walsh D, Mohr I.** 2011. Viral subversion of the host protein synthesis machinery.  
726 *Nature reviews Microbiology* **9**:860-875.
- 727 12. **Paranjape SM, Harris E.** 2010. Control of dengue virus translation and  
728 replication. *Curr Top Microbiol Immunol* **338**:15-34.
- 729 13. **Screaton G, Mongkolsapaya J, Yacoub S, Roberts C.** 2015. New insights into  
730 the immunopathology and control of dengue virus infection. *Nat Rev Immunol*  
731 **15**:745-759.

- 732 14. **Diamond MS, Pierson TC.** 2015. Molecular Insight into Dengue Virus  
733 Pathogenesis and Its Implications for Disease Control. *Cell* **162**:488-492.
- 734 15. **Edgil D, Polacek C, Harris E.** 2006. Dengue virus utilizes a novel strategy for  
735 translation initiation when cap-dependent translation is inhibited. *J Virol* **80**:2976-  
736 2986.
- 737 16. **Pena J, Harris E.** 2011. Dengue virus modulates the unfolded protein response  
738 in a time-dependent manner. *J Biol Chem* **286**:14226-14236.
- 739 17. **Dong H, Fink K, Zust R, Lim SP, Qin CF, Shi PY.** 2014. Flavivirus RNA  
740 methylation. *J Gen Virol* **95**:763-778.
- 741 18. **Mukhopadhyay S, Kuhn RJ, Rossmann MG.** 2005. A structural perspective of  
742 the flavivirus life cycle. *Nat Rev Microbiol* **3**:13-22.
- 743 19. **Cologna R, Rico-Hesse R.** 2003. American genotype structures decrease  
744 dengue virus output from human monocytes and dendritic cells. *J Virol* **77**:3929-  
745 3938.
- 746 20. **Klema VJ, Padmanabhan R, Choi KH.** 2015. Flaviviral Replication Complex:  
747 Coordination between RNA Synthesis and 5'-RNA Capping. *Viruses* **7**:4640-  
748 4656.
- 749 21. **Gamarnik AV, Andino R.** 1998. Switch from translation to RNA replication in a  
750 positive-stranded RNA virus. *Genes & development* **12**:2293-2304.
- 751 22. **Villordo SM, Filomatori CV, Sanchez-Vargas I, Blair CD, Gamarnik AV.** 2015.  
752 Dengue virus RNA structure specialization facilitates host adaptation. *PLoS*  
753 *pathogens* **11**:e1004604.
- 754 23. **Villordo SM, Alvarez DE, Gamarnik AV.** 2010. A balance between circular and  
755 linear forms of the dengue virus genome is crucial for viral replication. *RNA*  
756 **16**:2325-2335.
- 757 24. **Stohlman SA, Wisseman CL, Jr., Eylar OR, Silverman DJ.** 1975. Dengue  
758 virus-induced modifications of host cell membranes. *J Virol* **16**:1017-1026.
- 759 25. **Miller S, Sparacio S, Bartenschlager R.** 2006. Subcellular localization and  
760 membrane topology of the Dengue virus type 2 Non-structural protein 4B. *J Biol*  
761 *Chem* **281**:8854-8863.
- 762 26. **Heaton NS, Mosca F, Fenouil R, Gardner TJ, Aguirre S, Shah PS, Zhou N,**  
763 **Manganaro L, Hultquist JF, Noel J, Sachs DH, Hamilton J, Leon PE,**  
764 **Chawdury A, Tripathi S, Melegari C, Campisi L, Hai R, Meteveli G, Gamarnik**  
765 **AV, Garcia-Sastre A, Greenbaum B, Simon V, Fernandez-Sesma A, Krogan**  
766 **NJ, Mulder LC, van Bakel H, Tortorella D, Taunton J, Palese P, Marazzi I.**  
767 2016. Targeting Viral Proteostasis Limits Influenza Virus, HIV, and Dengue Virus  
768 Infection. *Immunity* **44**:46-58.
- 769 27. **Marceau CD, Puschnik AS, Majzoub K, Ooi YS, Brewer SM, Fuchs G,**  
770 **Swaminathan K, Mata MA, Elias JE, Sarnow P, Carette JE.** 2016. Genetic  
771 dissection of Flaviviridae host factors through genome-scale CRISPR screens.  
772 *Nature* **535**:159-163.
- 773 28. **Zhang R, Miner JJ, Gorman MJ, Rausch K, Ramage H, White JP, Zuiani A,**  
774 **Zhang P, Fernandez E, Zhang Q, Dowd KA, Pierson TC, Cherry S, Diamond**  
775 **MS.** 2016. A CRISPR screen defines a signal peptide processing pathway  
776 required by flaviviruses. *Nature* **535**:164-168.

- 777 29. **Staudacher JJ, Naarmann-de Vries IS, Ujvari SJ, Klinger B, Kasim M, Benko**  
778 **E, Ostareck-Lederer A, Ostareck DH, Bondke Persson A, Lorenzen S, Meier**  
779 **JC, Bluthgen N, Persson PB, Henrion-Caude A, Mrowka R, Fahling M.** 2015.  
780 Hypoxia-induced gene expression results from selective mRNA partitioning to the  
781 endoplasmic reticulum. *Nucleic acids research* **43**:3219-3236.
- 782 30. **Reid DW, Nicchitta CV.** 2015. Diversity and selectivity in mRNA translation on  
783 the endoplasmic reticulum. *Nat Rev Mol Cell Biol* **16**:221-231.
- 784 31. **Reid DW, Nicchitta CV.** 2012. Primary Role for Endoplasmic Reticulum-bound  
785 Ribosomes in Cellular Translation Identified by Ribosome Profiling. *The Journal*  
786 *of Biological Chemistry* **287**:5518-5527.
- 787 32. **Stephens SB, Nicchitta CV.** 2008. Divergent regulation of protein synthesis in  
788 the cytosol and endoplasmic reticulum compartments of mammalian cells.  
789 *Molecular biology of the cell* **19**:623-632.
- 790 33. **Diehn M, Eisen MB, Botstein D, Brown PO.** 2000. Large-scale identification of  
791 secreted and membrane-associated gene products using DNA microarrays.  
792 *Nature genetics* **25**:58-62.
- 793 34. **Ingolia NT.** 2014. Ribosome profiling: new views of translation, from single  
794 codons to genome scale. *Nat Rev Genet* **15**:205-213.
- 795 35. **Ingolia NT, Ghaemmaghami S, Newman JR, Weissman JS.** 2009. Genome-  
796 wide analysis in vivo of translation with nucleotide resolution using ribosome  
797 profiling. *Science* **324**:218-223.
- 798 36. **Jagannathan S, Nwosu C, Nicchitta CV.** 2011. Analyzing mRNA localization to  
799 the endoplasmic reticulum via cell fractionation. *Methods in molecular biology*  
800 **714**:301-321.
- 801 37. **Inoue T, Tsai B.** 2013. How viruses use the endoplasmic reticulum for entry,  
802 replication, and assembly. *Cold Spring Harb Perspect Biol* **5**:a013250.
- 803 38. **Welsch S, Miller S, Romero-Brey I, Merz A, Bleck CK, Walther P, Fuller SD,**  
804 **Antony C, Krijnse-Locker J, Bartenschlager R.** 2009. Composition and three-  
805 dimensional architecture of the dengue virus replication and assembly sites. *Cell*  
806 *Host Microbe* **5**:365-375.
- 807 39. **Lerner RS, Seiser RM, Zheng T, Lager PJ, Reedy MC, Keene JD, Nicchitta**  
808 **CV.** 2003. Partitioning and translation of mRNAs encoding soluble proteins on  
809 membrane-bound ribosomes. *RNA* **9**:1123-1137.
- 810 40. **Jagannathan S, Hsu JC, Reid DW, Chen Q, Thompson WJ, Moseley AM,**  
811 **Nicchitta CV.** 2014. Multifunctional roles for the protein translocation machinery  
812 in RNA anchoring to the endoplasmic reticulum. *The Journal of biological*  
813 *chemistry* **289**:25907-25924.
- 814 41. **Jagannathan S, Nwosu C, Nicchitta CV.** 2011. Analyzing mRNA localization to  
815 the endoplasmic reticulum via cell fractionation. *Methods Mol Biol* **714**:301-321.
- 816 42. **Reid DW, Chen Q, Tay AS, Shenolikar S, Nicchitta CV.** 2014. The unfolded  
817 protein response triggers selective mRNA release from the endoplasmic  
818 reticulum. *Cell* **158**:1362-1374.
- 819 43. **Reid DW, Nicchitta CV.** 2012. Primary role for endoplasmic reticulum-bound  
820 ribosomes in cellular translation identified by ribosome profiling. *J Biol Chem*  
821 **287**:5518-5527.

- 822 44. **Stephens SB, Dodd RD, Brewer JW, Lager PJ, Keene JD, Nicchitta CV.**  
823 2005. Stable ribosome binding to the endoplasmic reticulum enables  
824 compartment-specific regulation of mRNA translation. *Mol Biol Cell* **16**:5819-  
825 5831.
- 826 45. **Stephens SB, Dodd RD, Lerner RS, Pyhtila BM, Nicchitta CV.** 2008. Analysis  
827 of mRNA partitioning between the cytosol and endoplasmic reticulum  
828 compartments of mammalian cells. *Methods Mol Biol* **419**:197-214.
- 829 46. **Stephens SB, Nicchitta CV.** 2008. Divergent regulation of protein synthesis in  
830 the cytosol and endoplasmic reticulum compartments of mammalian cells. *Mol*  
831 *Biol Cell* **19**:623-632.
- 832 47. **Junjhon J, Lausumpao M, Supasa S, Noisakran S, Songjaeng A, Saraithong**  
833 **P, Chaichoun K, Utaipat U, Keelapang P, Kanjanahaluethai A, Puttikhunt C,**  
834 **Kasinrerk W, Malasit P, Sittisombut N.** 2008. Differential modulation of prM  
835 cleavage, extracellular particle distribution, and virus infectivity by conserved  
836 residues at nonfurin consensus positions of the dengue virus pr-M junction.  
837 *Journal of virology* **82**:10776-10791.
- 838 48. **Liu ZY, Li XF, Jiang T, Deng YQ, Ye Q, Zhao H, Yu JY, Qin CF.** 2016. Viral  
839 RNA switch mediates the dynamic control of flavivirus replicase recruitment by  
840 genome cyclization. *Elife* **5**.
- 841 49. **Araujo PR, Yoon K, Ko D, Smith AD, Qiao M, Suresh U, Burns SC, Penalva**  
842 **LO.** 2012. Before It Gets Started: Regulating Translation at the 5' UTR. *Comp*  
843 *Funct Genomics* **2012**:475731.
- 844 50. **Gebhard LG, Filomatori CV, Gamarnik AV.** 2011. Functional RNA elements in  
845 the dengue virus genome. *Viruses* **3**:1739-1756.
- 846 51. **Iglesias NG, Gamarnik AV.** 2011. Dynamic RNA structures in the dengue virus  
847 genome. *RNA Biol* **8**:249-257.
- 848 52. **Irigoyen N, Firth AE, Jones JD, Chung BY, Siddell SG, Brierley I.** 2016. High-  
849 Resolution Analysis of Coronavirus Gene Expression by RNA Sequencing and  
850 Ribosome Profiling. *PLoS pathogens* **12**:e1005473.
- 851 53. **Firth AE, Blitvich BJ, Wills NM, Miller CL, Atkins JF.** 2010. Evidence for  
852 ribosomal frameshifting and a novel overlapping gene in the genomes of insect-  
853 specific flaviviruses. *Virology* **399**:153-166.
- 854 54. **Firth AE, Brierley I.** 2012. Non-canonical translation in RNA viruses. *J Gen Virol*  
855 **93**:1385-1409.
- 856 55. **Markoff L.** 1989. In vitro processing of dengue virus structural proteins: cleavage  
857 of the pre-membrane protein. *Journal of virology* **63**:3345-3352.
- 858 56. **Clum S, Ebner KE, Padmanabhan R.** 1997. Cotranslational membrane  
859 insertion of the serine proteinase precursor NS2B-NS3(Pro) of dengue virus type  
860 2 is required for efficient in vitro processing and is mediated through the  
861 hydrophobic regions of NS2B. *The Journal of biological chemistry* **272**:30715-  
862 30723.
- 863 57. **Pijlman GP, Funk A, Kondratieva N, Leung J, Torres S, van der Aa L, Liu**  
864 **WJ, Palmenberg AC, Shi PY, Hall RA, Khromykh AA.** 2008. A highly  
865 structured, nuclease-resistant, noncoding RNA produced by flaviviruses is  
866 required for pathogenicity. *Cell host & microbe* **4**:579-591.

- 867 58. **Manokaran G, Finol E, Wang C, Gunaratne J, Bahl J, Ong EZ, Tan HC,**  
868 **Sessions OM, Ward AM, Gubler DJ, Harris E, Garcia-Blanco MA, Ooi EE.**  
869 2015. Dengue subgenomic RNA binds TRIM25 to inhibit interferon expression for  
870 epidemiological fitness. *Science* **350**:217-221.
- 871 59. **Pyhtila B, Zheng T, Lager PJ, Keene JD, Reedy MC, Nicchitta CV.** 2008.  
872 Signal sequence- and translation-independent mRNA localization to the  
873 endoplasmic reticulum. *RNA* **14**:445-453.
- 874 60. **Diehn M, Bhattacharya R, Botstein D, Brown PO.** 2006. Genome-scale  
875 identification of membrane-associated human mRNAs. *PLoS genetics* **2**:e11.
- 876 61. **Arava Y, Boas FE, Brown PO, Herschlag D.** 2005. Dissecting eukaryotic  
877 translation and its control by ribosome density mapping. *Nucleic Acids Res*  
878 **33**:2421-2432.
- 879 62. **Rogers DW, Bottcher MA, Traulsen A, Greig D.** 2017. Ribosome reinitiation  
880 can explain length-dependent translation of messenger RNA. *PLoS Comput Biol*  
881 **13**:e1005592.
- 882 63. **Beckmann R, Spahn CM, Frank J, Blobel G.** 2001. The active 80S ribosome-  
883 Sec61 complex. *Cold Spring Harb Symp Quant Biol* **66**:543-554.
- 884 64. **Menetret JF, Hegde RS, Aguiar M, Gygi SP, Park E, Rapoport TA, Akey CW.**  
885 2008. Single copies of Sec61 and TRAP associate with a nontranslating  
886 mammalian ribosome. *Structure* **16**:1126-1137.
- 887 65. **Voorhees RM, Fernandez IS, Scheres SH, Hegde RS.** 2014. Structure of the  
888 mammalian ribosome-Sec61 complex to 3.4 Å resolution. *Cell* **157**:1632-1643.
- 889 66. **Pena J, Harris E.** 2012. Early dengue virus protein synthesis induces extensive  
890 rearrangement of the endoplasmic reticulum independent of the UPR and  
891 SREBP-2 pathway. *PLoS One* **7**:e38202.
- 892 67. **Pena J, Harris E.** 2011. Dengue virus modulates the unfolded protein response  
893 in a time-dependent manner. *The Journal of biological chemistry* **286**:14226-  
894 14236.
- 895 68. **Perera R, Kuhn RJ.** 2008. Structural proteomics of dengue virus. *Curr Opin*  
896 *Microbiol* **11**:369-377.
- 897 69. **Luo D, Xu T, Hunke C, Gruber G, Vasudevan SG, Lescar J.** 2008. Crystal  
898 structure of the NS3 protease-helicase from dengue virus. *J Virol* **82**:173-183.
- 899 70. **Chambers TJ, Nestorowicz A, Amberg SM, Rice CM.** 1993. Mutagenesis of  
900 the yellow fever virus NS2B protein: effects on proteolytic processing, NS2B-NS3  
901 complex formation, and viral replication. *J Virol* **67**:6797-6807.
- 902 71. **Falgout B, Pethel M, Zhang YM, Lai CJ.** 1991. Both nonstructural proteins  
903 NS2B and NS3 are required for the proteolytic processing of dengue virus  
904 nonstructural proteins. *J Virol* **65**:2467-2475.
- 905 72. **Umareddy I, Pluquet O, Wang QY, Vasudevan SG, Chevet E, Gu F.** 2007.  
906 Dengue virus serotype infection specifies the activation of the unfolded protein  
907 response. *Virology Journal* **4**:91.
- 908 73. **Walter P, Ron D.** 2011. The unfolded protein response: from stress pathway to  
909 homeostatic regulation. *Science* **334**:1081-1086.
- 910 74. **Iwakoshi NN, Lee AH, Vallabhajosyula P, Otipoby KL, Rajewsky K, Glimcher**  
911 **LH.** 2003. Plasma cell differentiation and the unfolded protein response intersect  
912 at the transcription factor XBP-1. *Nat Immunol* **4**.

- 913 75. **Han J, Kaufman RJ.** 2017. Physiological/pathological ramifications of  
914 transcription factors in the unfolded protein response. *Genes Dev* **31**:1417-1438.
- 915 76. **Ron D, Walter P.** 2007. Signal integration in the endoplasmic reticulum unfolded  
916 protein response. *Nat Rev Mol Cell Biol* **8**:519-529.
- 917 77. **Schroder M, Kaufman RJ.** 2005. The mammalian unfolded protein response.  
918 *Annu Rev Biochem* **74**:739-789.
- 919 78. **Bidet K, Garcia-Blanco MA.** 2014. Flaviviral RNAs: weapons and targets in the  
920 war between virus and host. *The Biochemical journal* **462**:215-230.
- 921 79. **Ron D, Walter P.** 2007. Signal integration in the endoplasmic reticulum unfolded  
922 protein response. *Nature reviews Molecular cell biology* **8**:519-529.
- 923 80. **Chen Q, Jagannathan S, Reid DW, Zheng T, Nicchitta CV.** 2011. Hierarchical  
924 regulation of mRNA partitioning between the cytoplasm and the endoplasmic  
925 reticulum of mammalian cells. *Molecular Biology of the Cell* **22**:2646-2658.
- 926 81. **Cui XA, Palazzo AF.** 2014. Localization of mRNAs to the endoplasmic reticulum.  
927 *Wiley interdisciplinary reviews RNA* doi:10.1002/wrna.1225.
- 928 82. **Iglesias NG, Gamarnik AV.** 2011. Dynamic RNA structures in the dengue virus  
929 genome. *RNA biology* **8**:249-257.
- 930 83. **Irigoyen N, Firth AE, Jones JD, Chung BY, Siddell SG, Brierley I.** 2016. High-  
931 Resolution Analysis of Coronavirus Gene Expression by RNA Sequencing and  
932 Ribosome Profiling. *PLoS Pathog* **12**:e1005473.
- 933 84. **Lerner RS, Nicchitta CV.** 2006. mRNA translation is compartmentalized to the  
934 endoplasmic reticulum following physiological inhibition of cap-dependent  
935 translation. *RNA* **12**:775-789.
- 936 85. **Roth H, Magg V, Uch F, Mutz P, Klein P, Haneke K, Lohmann V,  
937 Bartenschlager R, Fackler OT, Locker N, Stoecklin G, Ruggieri A.** 2017.  
938 Flavivirus Infection Uncouples Translation Suppression from Cellular Stress  
939 Responses. *MBio* **8**.
- 940 86. **Li S, Liu L, Zhuang X, Yu Y, Liu X, Cui X, Ji L, Pan Z, Cao X, Mo B, Zhang F,  
941 Raikhel N, Jiang L, Chen X.** 2013. MicroRNAs inhibit the translation of target  
942 mRNAs on the endoplasmic reticulum in Arabidopsis. *Cell* **153**:562-574.
- 943 87. **Stalder L, Heusermann W, Sokol L, Trojer D, Wirz J, Hean J, Fritzsche A,  
944 Aeschimann F, Pfanzagl V, Basselet P, Weiler J, Hintersteiner M, Morrissey  
945 DV, Meisner-Kober NC.** 2013. The rough endoplasmic reticulum is a central  
946 nucleation site of siRNA-mediated RNA silencing. *EMBO J* **32**:1115-1127.
- 947 88. **Jagannathan S, Hsu JC, Reid DW, Chen Q, Thompson WJ, Moseley AM,  
948 Nicchitta CV.** 2014. Multifunctional roles for the protein translocation machinery  
949 in RNA anchoring to the endoplasmic reticulum. *J Biol Chem* **289**:25907-25924.
- 950 89. **Stephens SB, Nicchitta CV.** 2007. In vitro and tissue culture methods for  
951 analysis of translation initiation on the endoplasmic reticulum. *Methods Enzymol*  
952 **431**:47-60.
- 953 90. **Reid DW, Shenolikar S, Nicchitta CV.** 2015. Simple and inexpensive ribosome  
954 profiling analysis of mRNA translation. *Methods*  
955 doi:10.1016/j.ymeth.2015.07.003.
- 956 91. **Martin M.** 2011. Cutadapt removes adapter sequences from high-throughput  
957 sequencing reads. *EMBnetjournal* **17**:10-12.

- 958 92. **Pollier J, Rombauts S, Goossens A.** 2013. Analysis of RNA-Seq data with  
959 TopHat and Cufflinks for genome-wide expression analysis of jasmonate-treated  
960 plants and plant cultures. *Methods Mol Biol* **1011**:305-315.
- 961 93. **Langmead B, Trapnell C, Pop M, Salzberg SL.** 2009. Ultrafast and memory-  
962 efficient alignment of short DNA sequences to the human genome. *Genome*  
963 *biology* **10**:R25.
- 964 94. **Jovanovic M, Rooney MS, Mertins P, Przybylski D, Chevrier N, Satija R,**  
965 **Rodriguez EH, Fields AP, Schwartz S, Raychowdhury R, Mumbach MR,**  
966 **Eisenhaure T, Rabani M, Gennert D, Lu D, Delorey T, Weissman JS, Carr**  
967 **SA, Hacohen N, Regev A.** 2015. Immunogenetics. Dynamic profiling of the  
968 protein life cycle in response to pathogens. *Science* **347**:1259038.
- 969

970 **Figure Legends**

971 **Figure 1. Experimental schematic and validation of cell fractionation protocol. A)**

972 Schematic of the experimental approach. Mock- or DEV-infected Huh7 cells were  
973 fractionated by a sequential detergent extraction protocol where cell cultures are first  
974 treated with digitonin-supplemented buffers to release the cytosolic contents followed by  
975 a subsequent treatment with dodecylmaltoside (DDM)-supplemented buffers to release  
976 the ER-associated contents. Total RNA was isolated from each fraction and analyzed  
977 by RNA-Seq to assess gene expression. In parallel, polysomes in each fraction were  
978 nuclease digested, ribosome footprints isolated, and analyzed by Ribo-Seq. **B)**  
979 Immunoblot analysis of the distributions of cytosolic (GAPDH and tubulin) and ER  
980 resident membrane (Ribophorin I and TRAP $\alpha$ ) proteins in the cytosol (Cyt) and ER  
981 fractions of mock-infected cells and following 40 h of DENV infection (MOI = 10). **C)**  
982 Ribosome and tRNA distributions in the two subcellular fractions were determined by  
983 isolation of total RNA, separation by agarose gel electrophoresis, and visualization with  
984 SYBR Green staining. 18S, 28S and tRNA components are indicated.

985

986 **Figure 2. Spatiotemporal organization of DENV replication and translation. A)**

987 Abundance of DENV (+) and (-) RNA over a 40 h infection time course, as assessed by  
988 RNA-seq. **B)** Rate of accumulation for DENV (+) and (-) RNA. Each point indicates the  
989 average rate of change of RNA abundance between the two adjacent time points,  
990 expressed as percent change per hour in an exponential growth model. **C)** Percentage  
991 of DENV + strand RNA, - strand RNA, and + strand translation that is ER-associated  
992 throughout the experimental time course. **D)** Translational efficiency of DENV RNA

993 relative to the host transcriptome. The translation efficiency distributions of host mRNAs  
994 encoding TMHMM-predicted ER-targeted proteins is shown in black, with the translation  
995 efficiency of DENV RNA in red. The translation efficiency distribution is calculated as an  
996 average value of all mRNAs at all time points. For all panels, error bars represent  $\pm$ SD  
997 (n=2).

998 **Figure 3. Ribosome footprinting pattern of the DENV RNA. A)** Ribosome density  
999 across the DENV RNA at each infection time point as a 30-nt moving window. Red lines  
1000 separate different coding sequences, while the grey area indicates the entire polyprotein  
1001 coding sequence. **B)** Schematic representation of the DENV polyprotein with each  
1002 protein color-coded as legend for panel **C**. **C)** Ribosome density for each viral protein  
1003 coding region over the course of infection (color legend, panel **B**).

1004 **Figure 4. sfRNA abundance and subcellular localization. A)** RNA-seq read density  
1005 in the cytosol and ER fractions along the DENV RNA sequence. The coding sequence  
1006 is indicated by the grey shaded area and different coding sequences by red lines. The  
1007 sfRNA is derived from the DENV 3' UTR. **B)** Subcellular localization of the sfRNA  
1008 relative to the (+) strand DENV RNA. **C)** Distribution of read lengths for ribosome  
1009 profiling reads mapping to the transcriptome, DENV coding sequence, and DENV 3'  
1010 UTR.

1011 **Figure 5. DENV selectively remodels the ER translational landscape. A)** Change in  
1012 the total translation of mRNAs over the infection time course, as assessed by ribosome  
1013 footprinting. Two categories of mRNAs are plotted: mRNAs encoding ER-targeted  
1014 proteins, which encode a signal sequence or transmembrane domain, and mRNAs

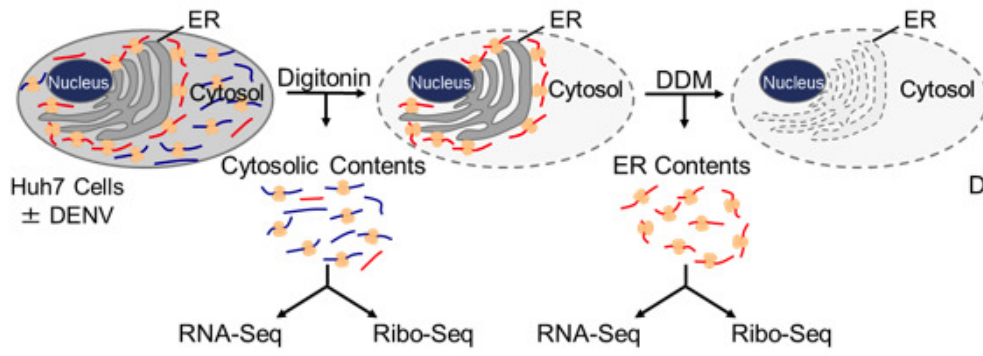
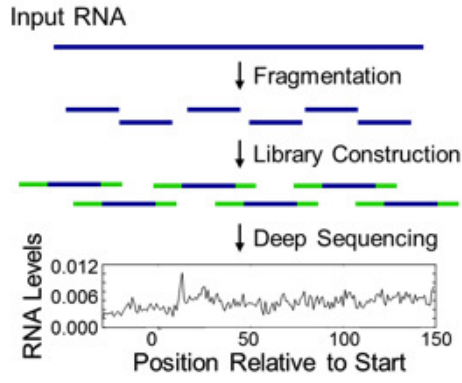
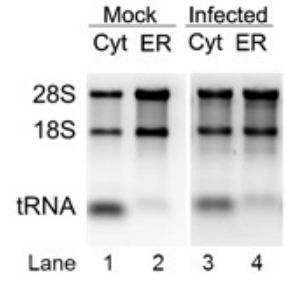
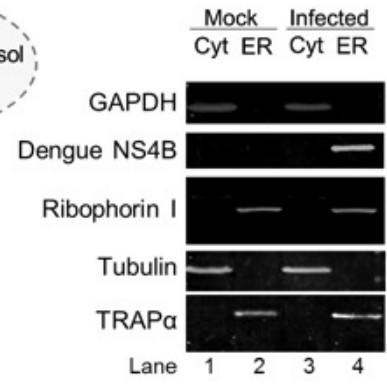
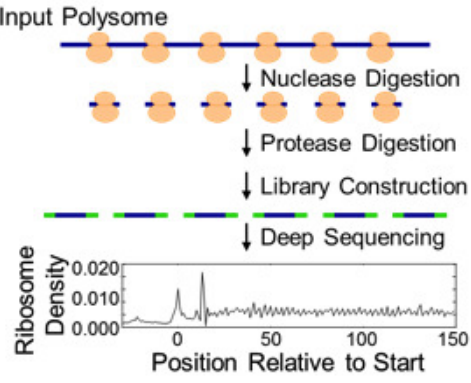
1015 encoding cytosolic proteins, which do not. Total translation was measured as the total  
1016 number of ribosome footprinting reads mapped to an mRNA cohort, normalized for  
1017 library size, and then expressed as a percentage of that value in mock infected cells.  
1018 DENV RNAs were excluded from these calculations. **B)** As in A, except mRNA levels  
1019 are depicted, as measured by RNA-seq and normalized to length. **C)** Time course of  
1020 ribosome recruitment by ER-associated DENV (+) RNA. Illustrated is the fractional  
1021 capture of ER-bound ribosomes translating topogenic signal-encoding mRNAs (signal  
1022 sequence and/or transmembrane domains, i.e. ER-targeted host mRNA) and DENV (+)  
1023 RNA, as determined from the Ribo-seq datasets. Ribosome abundance is calculated as  
1024 RPKM x CDS length x  $10^6$ . **D)** Fraction of ER-bound ribosomes translating non-  
1025 topogenic signal-encoding mRNAs (i.e. cytosol-encoding host mRNA) and DENV (+)  
1026 RNA, as calculated in **4C**. **E)** Metabolic labeling of newly-synthesized total, ER-  
1027 associated and cytosolic proteins. Cells were infected with DENV for 36 h then pulse-  
1028 labeled with [ $^{35}\text{S}$ ]Met/Cys. Cells were either directly detergent extracted (Total) or  
1029 fractionated as in illustrated in Fig.1 to obtain ER and cytosol (Cyt) fractions and  
1030 analyzed by SDS-PAGE followed by autoradiography. Bands appearing samples from  
1031 the DENV infected samples are presumed to be DENV proteins and are labeled based  
1032 on known molecular weight. **F)** Immunoblot analyses of a subset of DENV proteins  
1033 confirms expression and subcellular distributions indicated in panel E.

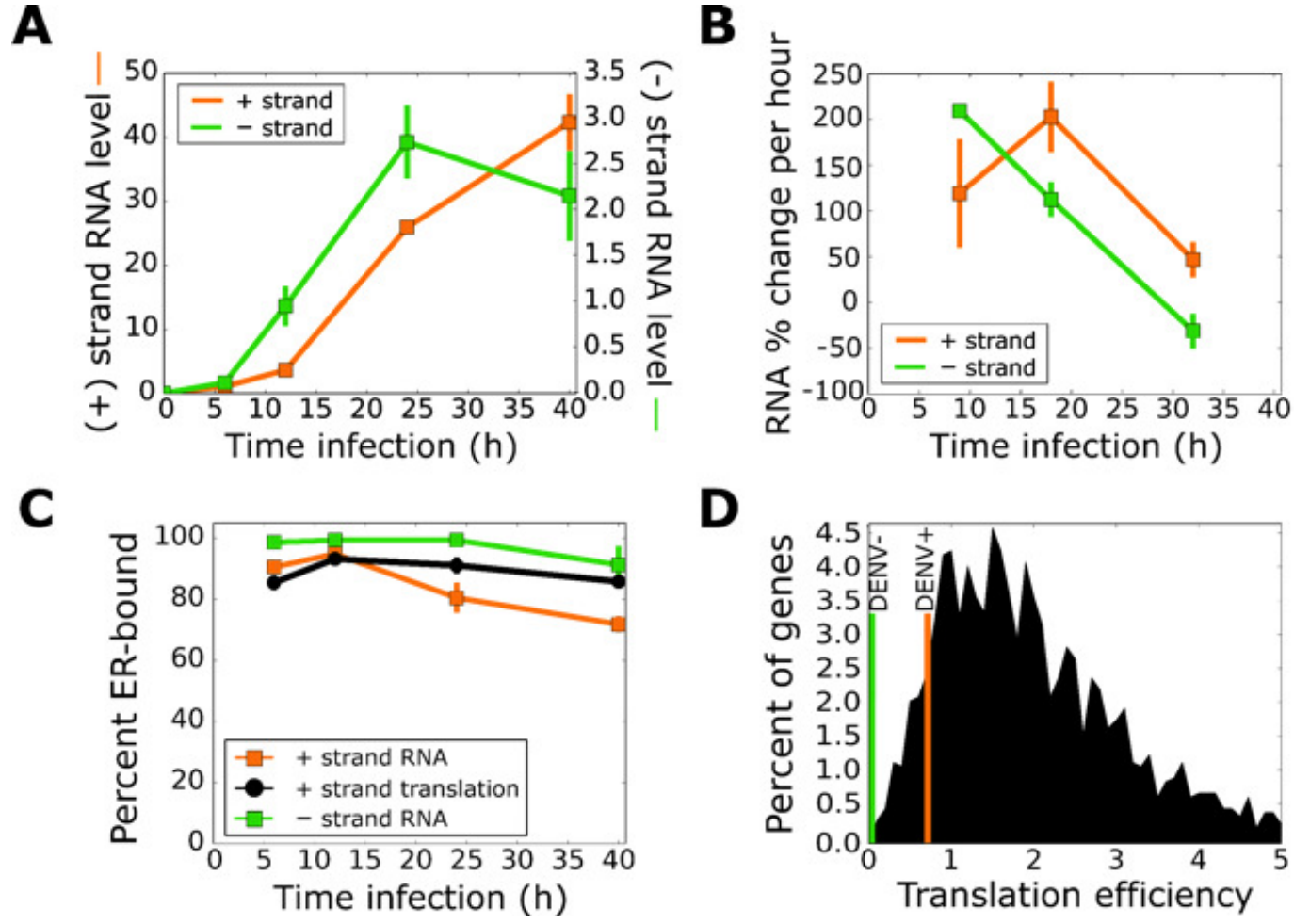
1034

1035 **Figure 6. Host gene expression response to DENV infection.** **A)** Heat map of  
1036 changes in total translation of host genes over the DENV infection time course. Genes  
1037 are sorted by their mean response over the time course of infection. The translational

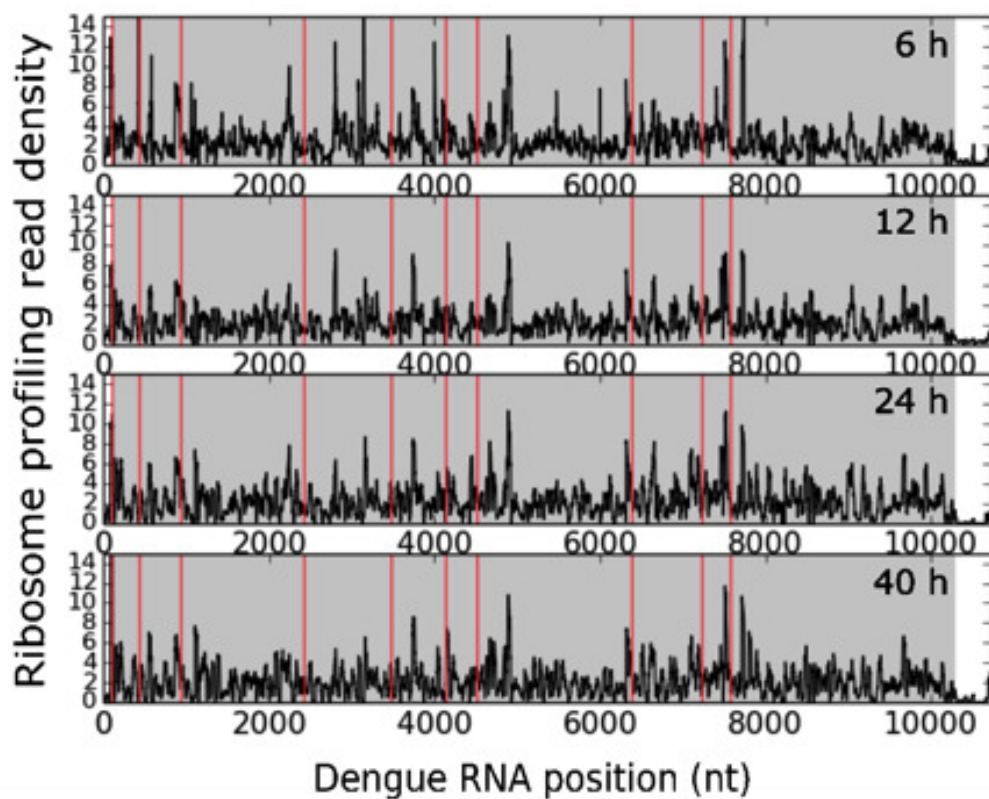
1038 response to interferon beta 1A treatment is also indicated. **B)** Changes during DENV  
1039 infection in the interferon-induced-only gene set (defined as those genes increased at  
1040 least 50% after treatment with interferon beta 1A) and the UPR-induced gene set  
1041 (genes increased at least 50% after 4 h UPR induction)(UPR gene set from (42)). **C)**  
1042 Venn diagram specifying the overlaps between the interferon and UPR gene sets  
1043 described above and the genes increased at least 100% in total translation after 40 h  
1044 DENV infection. **D)** Five most significant gene ontology terms for DENV-only gene set  
1045 determined for biological process using GOrilla with the full data set as the background  
1046 list. **E)** The contributions of changes in mRNA levels and translational efficiency to  
1047 changes in total translational activity after 40 h DENV infection. These values were  
1048 calculated as described in Materials and Methods for all genes and for each set of  
1049 genes that is exclusively identified as DENV, UPR, or IFN.

1050 **Figure 7. Translational changes of CRISPR-identified host factors during DENV**  
1051 **infection. A)** Histogram showing changes in total translation for CRISPR-identified  
1052 essential genes for DENV2 as determined in Marceau, et al. (27). Genes that were  
1053 essential for DENV replication and with a RIGER score of > 1 were operationally scored  
1054 as essential, while all other genes were scored as non-essential. **B)** List of log<sub>2</sub> change  
1055 in translation for CRISPR-identified essential genes for DENV2 as determined in  
1056 Marceau, et al. (27), with RIGER score of > 1, after 40 h infection. These values were  
1057 calculated as described in Materials and Methods. The ER-localization status of each  
1058 gene product is also indicated.

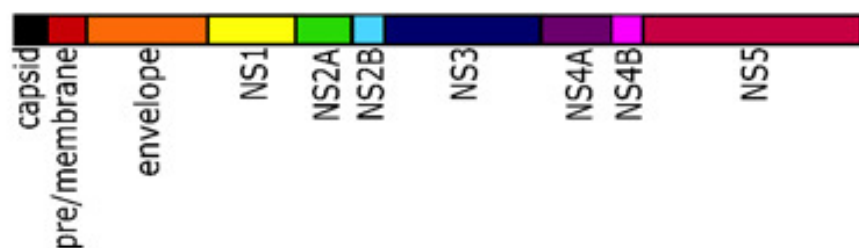
**RNA-Seq Outline:****Ribo-Seq Outline:**



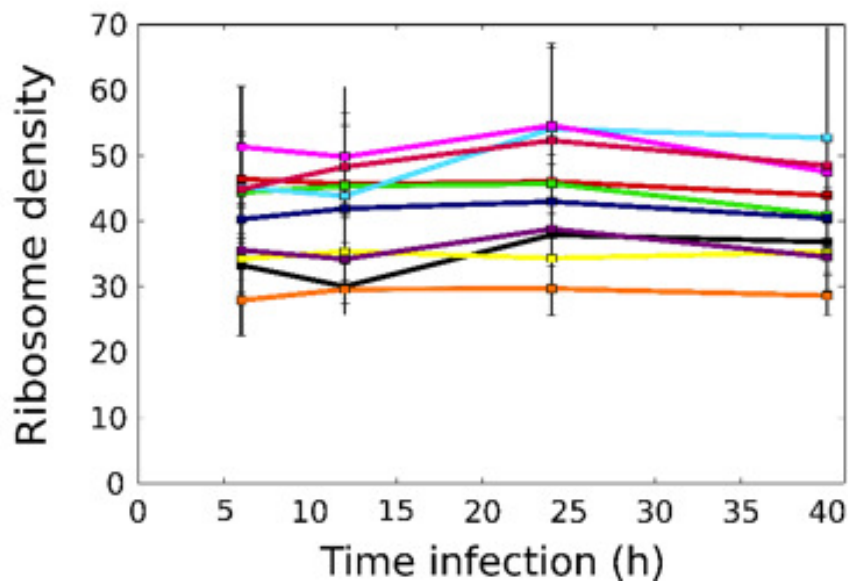
**A**

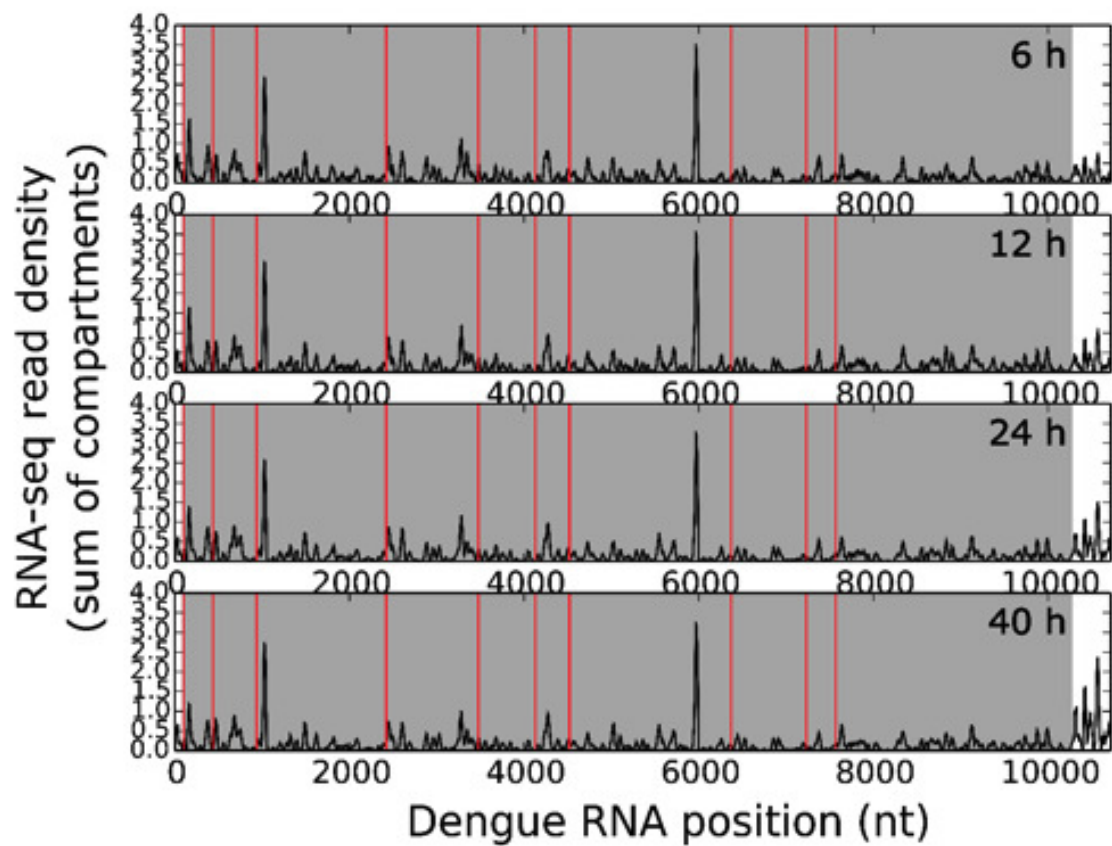
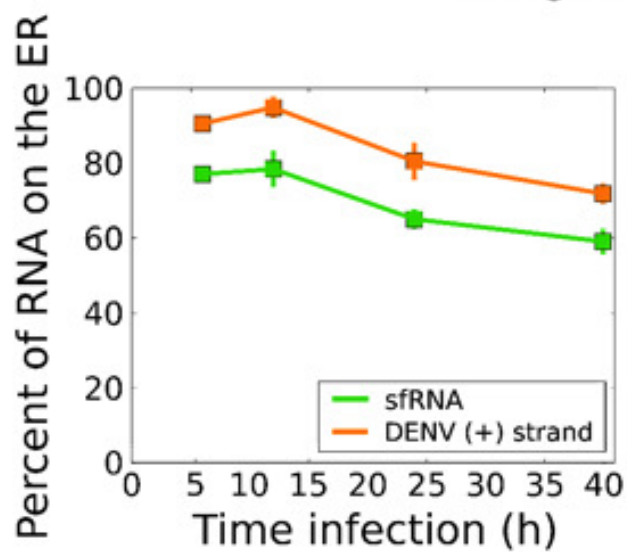
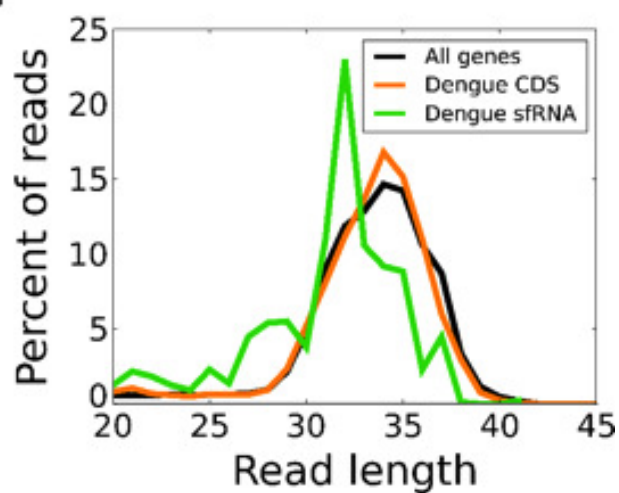


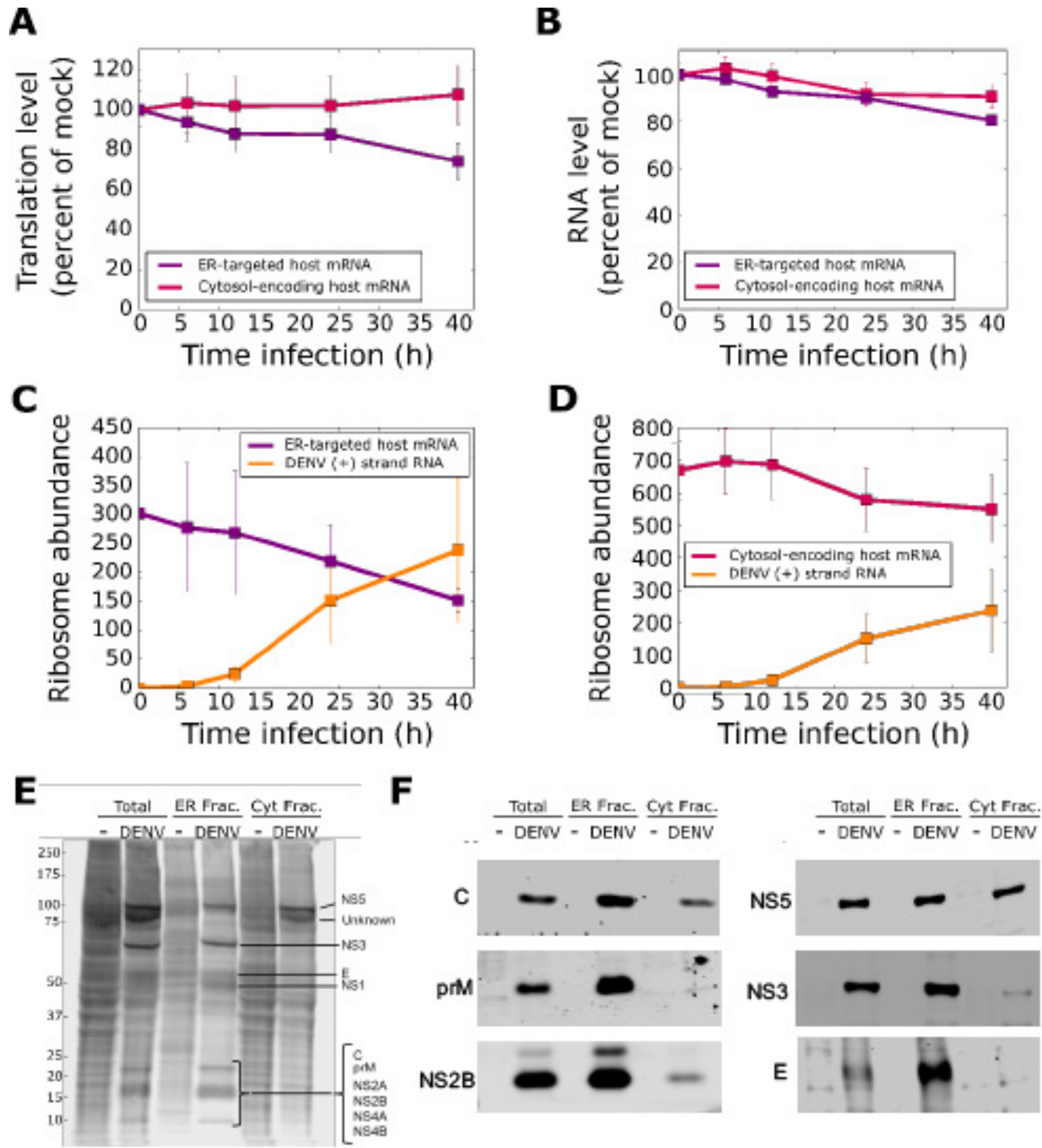
**B**

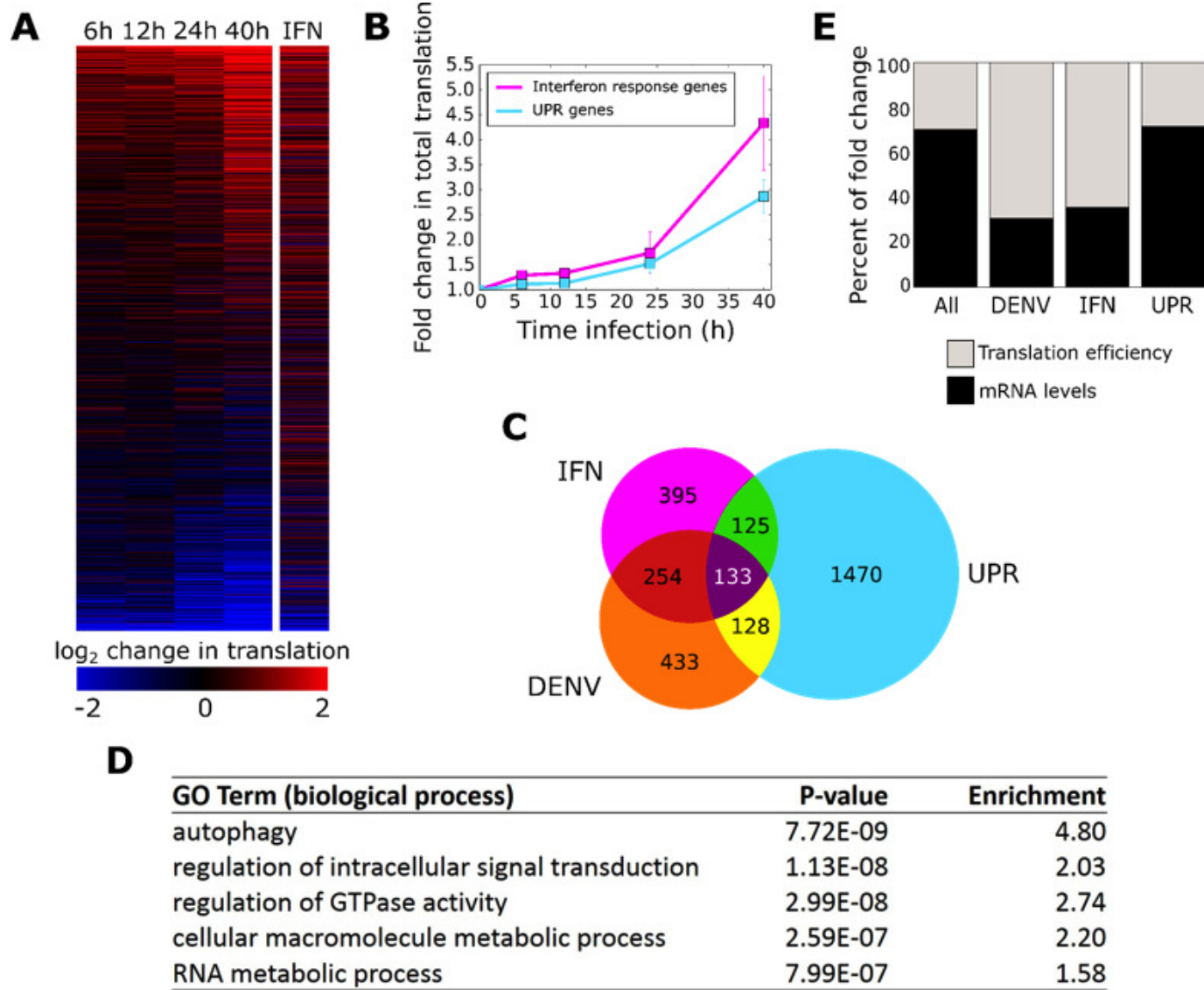


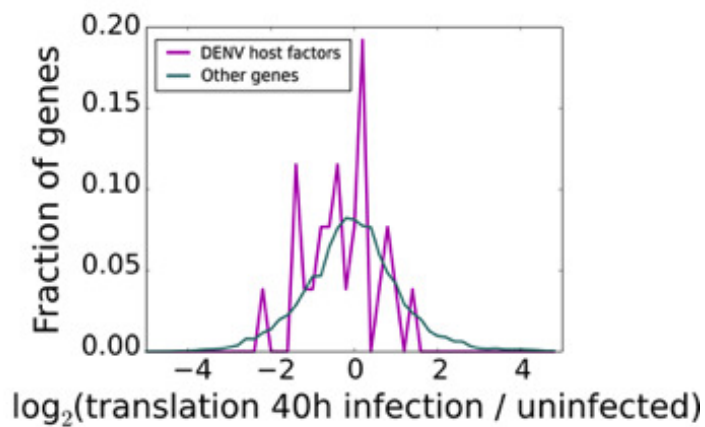
**C**



**A****B****C**





**A****B**

Gene ID	ER?	Log <sub>2</sub> change in total translation
CILP	No	NA
NRSN1	Yes	NA
EMC2	Yes	2.561466
TBC1D9	Yes	1.646808
TSEN15	No	1.175835
RAB5A	No	1.153792
ASCC2	No	1.129517
TTC7A	No	1.105917
LYSMD3	Yes	1.016606
ASCC3	No	0.560635
UBE2J1	Yes	0.084272
SSR3	Yes	0.02432
HSPA13	Yes	0.001863
OST4	Yes	-0.13629
MAGT1	Yes	-0.27337
SSR2	Yes	-0.36101
TTC37	No	-0.38785
SEC61A1	Yes	-0.4794
EMC3	Yes	-0.57981
LEPROT	No	-0.57992
EMC6	Yes	-0.58141
OSTC	Yes	-0.60656
DDOST	Yes	-0.74725
EMC7	Yes	-0.75134
SSR1	Yes	-0.80355
STT3A	Yes	-0.97432
SAMD8	Yes	-1.11429
MMGT1	Yes	-1.14545
EMC1	Yes	-1.20918
RPN2	Yes	-1.31322
EMC4	Yes	-1.34744
STT3B	Yes	-1.46459
SVEP1	No	-1.49111
DAG1	No	-2.31305

2

log<sub>2</sub> change in translation

-2